Titre: Title:	Simultaneous Manganese Removal and Remineralization of Soft Waters Via Calcite Contactor
Auteur: Author:	Hamed Pourahmad
Date:	2018
Type:	Mémoire ou thèse / Dissertation or Thesis
Référence: Citation:	Pourahmad, H. (2018). Simultaneous Manganese Removal and Remineralization of Soft Waters Via Calcite Contactor [Mémoire de maîtrise, École Polytechnique de Montréal]. PolyPublie. https://publications.polymtl.ca/3702/

UNIVERSITÉ DE MONTRÉAL

Simultaneous Manganese Removal and Remineralization Of Soft Waters Via Calcite Contactor

HAMED POURAHMAD

DÉPARTEMENT DES GÉNIES CIVIL, GÉOLOGIQUE ET DES MINES (CGM)

ÉCOLE POLYTECHNIQUE DE MONTRÉAL

MÉMOIRE PRÉSENTÉ EN VUE DE L'OBTENTION
DU DIPLÔME DE MAÎTRISE ÈS SCIENCES APPLIQUÉES
(GÉNIE CIVIL)

DÉCEMBRE 2018

UNIVERSITÉ DE MONTRÉAL

ÉCOLE POLYTECHNIQUE DE MONTRÉAL

Ce mémoire intitulé :

Simultaneous Manganese Removal and Remineralization Of Soft Waters Via Calcite Contactor

Présenté par : POURAHMAD, Hamed

En vue de l'obtention du diplôme de : Maîtrise ès sciences appliquées

A été dûment accepté par le jury d'examen constitué de :

M. COMEAU, Yves, Ph. D., président

M. BARBEAU, Benoit, Ph. D., membre et directeur de recherche

Mme. VANEECKHAUTE, Céline, Ph.D., membre

DEDICATION

To my beloved family, for their ineffable love, care and support...

ACKNOWLEDGEMENTS

I would like to express my sincere gratitude to my research director Professor Benoit Barbeau, for his continues support and guidance throughout my master's study. His patience and immense knowledge helped me in all the time. The door to Prof. Barbeau's office was always open whenever I ran into a trouble spot or had a question about my research or writing. I would like to thank you for all the priceless advices and for giving me the great opportunity of being a part of your team.

I acknowledge the members of my committee, Professor Yves Comeau and Professor Céline Vaneeckhaute for taking interest in my work and examining my thesis.

My special thanks to my mentor Maryam Haddad. I learned so much from you in each step of this project. I deeply appreciate your presence from the very beginning of the project.

My sincere gratitude goes to Dominique Claveau-Mallet for helping me in doing the modeling part of this work and offering her time and valuable technical advices. I truly appreciate her professionalism.

I also gratefully acknowledge the financial support by the Canadian NSERC Discovery Grant Program which made this research work possible.

My deepest appreciation goes to the technicians and research associates in the Department of Civil, Geological and Mining Engineering, particularly Mireille, Gabriel, Yves, Julie and Jacinthe for their excellent assistance. In addition, I thank the secretary of the Department of Civil, Geological and Mining Engineering for helping us and providing us with an ideal atmosphere.

Special thanks to my Polytechnique friends, Sanaz, Saber and Nargess. I am very grateful to all my colleagues in our research group and my fellow labmates and officemates for their cooperative manner and friendly support.

Finally, I would like to express my ineffable gratitude to my mother, lovely brothers and sisters, and in-laws for their solid support and undoubtedly, I would not have finished my thesis without their support.

RÉSUMÉ

Les eaux souterraines représentent 96% de l'approvisionnement en eau douce non gelée et fournissent près de la moitié de l'approvisionnement en eau potable dans le monde. En Amérique du Nord, environ 28% des Canadiens et 44% de la population américaine, vivant principalement en zone rurale, dépendent des eaux souterraines pour leur principale source d'approvisionnement en eau. Des concentrations élevées de manganèse (Mn) existent souvent naturellement dans les eaux souterraines (Civardi & Tompeck, 2015). Bien que la présence de manganèse dans l'eau potable pose des problèmes d'ordre esthétique et opérationnel, (Bouchard et al., 2011) ont indiqué que la consommation d'eau très concentrée en manganèse entraînait une déficience intellectuelle et des désordres neurologiques chez les enfants d'âge scolaire. Par conséquent, Santé Canada (2016) a récemment proposé une limite fondée sur la santé pour protéger les enfants des effets neurotoxiques. La filtration catalytique ou l'échange ionique cationique couplée aux procédés d'osmose inverse au point d'utilisation sont largement utilisés pour éliminer le manganèse et le fer des eaux souterraines. Cependant, le risque de lessivage du manganèse par des filtres catalytiques mal opérés, une consommation élevée de sel pour la régénération par échange d'ions et une quantité considérable de déchets de saumure, polluante pour l'environnement, sont des inconvénients courants de ces méthodes. En guise d'alternative, l'application du procédé de membrane de nanofiltration à fibres creuses (HFNF) a récemment été proposée pour traiter les sources d'approvisionnement en eau souterraine domestiques dans les petites communautés/régions isolées ou même pour des applications domestiques pour lesquelles les ressources financières et techniques disponibles sont une préoccupation importante lors du choix des solutions. Même si l'application d'un procédé membranaire peut constituer une solution attrayante pour une élimination efficace du manganèse, du fer et des agents pathogènes, la propriété non sélective des membranes de nanofiltration (NF) peut entraîner l'appauvrissement des niveaux de dureté et d'alcalinité des eaux souterraines et, par la suite, une eau traitée corrosive. Par conséquent, le procédé à membrane de nanofiltration doit être associé à une étape de polissage, tel qu'un contacteur de calcite ($CaCO_3$), pour ajuster le niveau de dureté de son perméat. En outre, un autre avantage intéressant de la calcite réside dans sa capacité à adsorber des cations métalliques divalents à sa surface (Aziz & Smith, 1996; Franklin & Morse, 1983). Ainsi, développer un procédé capable d'éliminer efficacement les résidus de manganèse du procédé de nanofiltration (qui n'est pas nécessairement totalement rejeté à cette étape) tout en ajoutant de la dureté à l'eau traitée est d'un grand intérêt.

L'objectif principal de ce projet de recherche est de concevoir une étape de polissage simple, mais robuste, capable d'ajuster le niveau de dureté (minimum cible de 40 mg $CaCO_3$ L^{-1}) et d'éliminer les traces de manganèse de l'eau douce (limite cible de 0,02 mg Mn L^{-1}). De manière plus détaillée, les objectifs spécifiques suivants sont définis: (1) déterminer le rôle des spécifications du support (utilisation de calcite pure ou d'un mélange de calcite et de Corosex^{TM} (MgO)), (2) sélectionner les meilleures conditions pour un fonctionnement efficace d'un contacteur de calcite comme étape de polissage (e.g. température, EBCT), (3) étudier la signification et le devenir du manganèse sorbé sur les performances globales d'un contacteur de calcite en fonctionnement à long terme et (4)

modéliser le comportement à long terme d'un contacteur de calcite utilisé pour la reminéralisation de l'eau potable.

Dans la première phase de ce projet, la performance globale d'un contacteur de calcite pour l'élimination du manganèse et la reminéralisation de l'eau douce en utilisant deux concentrations initiales de manganèse (e.g. 0,5 et 5 mg Mn L-1) a été étudiée. Le contacteur de calcite a démontré une efficacité élevée d'élimination du manganèse (moins de 20 µg Mn / L dans l'effluent); toutefois, la libération de dureté a diminué de 32 à 20 mg de $CaCO_3$ L^{-1} après 600 h de fonctionnement dans des conditions de concentration élevée en manganèse. Sur la base des résultats, dans la deuxième phase, l'impact négatif de la couche de manganèse nouvellement formée sur la vitesse de dissolution de la calcite à l'aide d'expériences continues de désorption-dissolution dans des colonnes plus petites a été étudié. Pour une concentration élevée de manganèse (e.g. 5,0 mg Mn L^{-1}) dans l'eau d'alimentation, la couche formée était principalement composée de manganèse, qui inhibe le transfert de masse du noyau de calcite à la phase liquide. La couche superficielle a été identifiée à 5,2% d'oxydes de manganèse (MnO_x) par spectroscopie photoélectronique à rayons X (XPS). Par conséquent, il est postulé que l'élimination du Mn commence par une réaction de sorption d'échange d'ions entre le manganèse soluble de la phase aqueuse et le calcium de la matrice de calcite, suivie d'une recristallisation lente du carbonate de manganèse en oxyde de manganèse. D'autre part, lorsque la teneur en manganèse dans l'eau d'alimentation était inférieure (e.g. 0,5 mg Mn L^{-1}), une quantité considérablement inférieure de MnOx était détectée sur la calcite. Pour toutes les conditions examinées, la formation de ce revêtement améliorait l'élimination du manganèse en raison de la nature autocatalytique de l'adsorption/oxydation du manganèse dissous par MnOx. Quant à la troisième phase, l'efficacité à long terme d'un contacteur de calcite a été modélisée à l'aide d'un modèle mécaniste basé sur la dissolution de la calcite et la formation progressive d'une couche d'oxyde de manganèse, implémenté dans le logiciel PHREEQC à l'aide d'une interface MATLAB via des modules IPHREEQC afin de prédire la réduction dans la libération de dureté attendue en fonctionnement à long terme. Le modèle a été calibré avec des données expérimentales et a abouti à des courbes de percée réalistes. Afin de prédire avec précision le pH du flux d'effluent, une recristallisation à vitesse lente de $MnCO_3$ en MnO_2 a été posée (par rapport à une précipitation rapide de MnO_2 ou à l'absence de formation de MnO_2). Enfin, étant donné qu'après un fonctionnement prolongé du contacteur de calcite en présence de concentrations élevées de manganèse, l'objectif de reminéralisation n'a pas été pleinement atteint, une solution possible a été testée en utilisant un mélange de calcite et de *Corosex*^{TM} (MgO) comme moyen de filtration. À cette fin, un premier rapport optimal de 80% / 20% pour Calcite / *Corosex*^{TM} a été obtenu, puis la colonne a été exploitée avec une concentration de manganèse élevée (5 mg Mn L^{-1}) avec le rapport choisi pour étudier l'efficacité du contacteur en reminéralisation d'eau douce avec élimination simultanée du manganèse. La colonne a démontré une efficacité élevée: dans le fonctionnement à long terme, le contacteur a pu éliminer plus de 99% du manganèse dissous de l'eau d'alimentation synthétique et a ajouté plus de 40 mg de $CaCO_3$ L^{-1} de dureté à l'alimentation douce. La condition stable a été atteinte beaucoup plus tôt que lors de la phase précédente où seule la calcite était utilisée (10 h de

fonctionnement par rapport à plus de 200 h de fonctionnement). L'accumulation de résidus de Mn nouvellement formés a augmenté la perte de charge et entraîné l'encrassement du filtre. Il est important de noter que l'utilisation d'un mélange de calcite et de *Corosex* ne semble pas une option prometteuse pour une opération à long terme si la concentration de manganèse dans l'alimentation est trop élevée (e.g. 5 mg Mn L^{-1}). Cependant, pour des concentrations de Mn plus réalistes (e.g. 0,2 mg Mn L^{-1} et moins), l'ajout d'une petite portion de *Corosex* au filtre contribuerait à améliorer l'ajout de dureté.

ABSTRACT

Groundwater (GW) accounts for 96% of all unfrozen fresh water supply and provides nearly half of the world's drinking water supply. In North America, approximately 28% of Canadians and 44% of the United States population, mainly living in rural areas, rely on GW as their main water supply. High manganese (Mn) concentrations often naturally exist in GW (Civardi & Tompeck, 2015). Despite the fact that the presence of Mn in finished water causes aesthetic and operational issues, (Bouchard et al., 2011) reported that consumption of water with high Mn concentration led to significant intellectual impairment and neurological disorders in school-age children. Consequently, Health Canada (2016) has recently proposed a health-based limit to protect children from neurotoxic effects. Catalytic filtration or cationic ion exchange (IX) coupled with point-of-use reverse osmosis processes are widely implemented to remove Mn and Fe from GW. However, the risk of Mn leaching from improperly operated catalytic filters, high salt consumption for IX regeneration and a considerable amount of brine waste production, which pollutes the environment, are common drawbacks of these methods. As an alternative, the application of hollow fiber nanofiltration (HFNF) membrane process has been recently proposed for treating domestic GW supplies in small/remote communities or even for domestic applications where the financial and technical resources are important concerns. Even though the application of a membrane process can be an appealing solution for effective removal of Mn, Fe and pathogens, non-selective property of the HFNF membranes may result in depletion of GW hardness and alkalinity levels and subsequently, corrosive treated water. Therefore, the HFNF process should be coupled with a polishing step, such as calcite contactor, to adjust the hardness level of its soft permeate. Moreover, another interesting advantage of calcite lies in its ability to sorb divalent metallic cations (Me^{2+}) on its surface (Aziz & Smith, 1996; Franklin & Morse, 1983). Thus, developing a process which can efficiently remove the leftover of Mn from the NF process (which is not necessarily fully rejected in this step) while adding hardness to treated water is of great interest.

The main objective of this research project is to design a simple, yet robust polishing step which can adjust the hardness level (target minimum of 40 mg $CaCO_3$/L) and remove the traces of Mn from the soft water (target limit of 0.02 mg Mn/L). On a more detailed basis, the following specific objectives are defined: (1) determine the role of the media specifications (i.e., use of pure calcite ($CaCO_3$) or a blend of calcite and *Corosex*^{TM} (MgO)), (2) screen the best operational conditions for the efficient operation of a calcite contactor as a polishing step (i.e., temperature, EBCT), (3) investigate the significance and fate of sorbed Mn on the overall performance of a calcite contactor in long-term operation and (4) model the long-term behavior of a calcite contactor operated for drinking water remineralization.

In the first phase of this project, the overall performance of a calcite contactor for the removal of Mn and remineralization of soft water using two initial concentrations of Mn (i.e. 0.5 and 5 mg Mn L^{-1}) was investigated. The calcite contactor demonstrated high Mn removal efficiency (below 20 µg Mn/L in the effluent); however, the hardness release decreased from 32 to 20 mg $CaCO_3$ L^{-1} after 600 h of operation in high Mn concentration condition. Based on the results, in the second

phase, the negative impact of newly-formed Mn-layer on calcite dissolution rate using continuous desorption-dissolution experiments in smaller columns was investigated. For an elevated Mn concentration (i.e. 5.0 mg Mn L^{-1}) in the feed water, the coated layer was mainly composed of Mn which inhibits the mass transfer from the calcite core to the liquid phase. The superficial layer was identified as 5.2% Mn oxides (MnOx) by X-ray photoelectron spectroscopy (XPS). Therefore, it is postulated that Mn removal starts with an ion exchange sorption reaction between soluble Mn^{2+} from aqueous phase and Ca^{2+} from the $CaCO_3$ matrix which is followed by a slow recrystallization of $MnCO_3$ into MnO_2. On the other hand, when the Mn content in the feed water was lower (i.e. 0.5 mg Mn L^{-1}), a considerably lower amount of MnOx was detected on the coated media. For all the examined conditions, the formation of this coating improved Mn removal due to the autocatalytic nature of adsorption/oxidation of dissolved manganese by MnOx. As for the third phase, the long-term efficiency of a calcite contactor was modeled using a mechanistic model based on calcite dissolution and progressive formation of a MnO_2 layer which was implemented in PHREEQC software using a MATLAB interface via IPHREEQC modules to predict the reduction in hardness release expected in long-term operation. The model was calibrated with experimental data and resulted in realistic breakthrough curves. In order to accurately predict the pH of the effluent stream, a slow-rate recrystallization of $MnCO_3$ into MnO_2 was implemented (compared to fast precipitation of MnO_2 or absence of MnO_2 formation). Finally, given that after long-term operation of the calcite contactor in elevated Mn concentrations, the remineralization objective was not fully met, a possible solution was tested using a blend of calcite and *Corosex*^{TM} (MgO) as the filtration media. For this purpose, first optimum ratio of 80% / 20% for Calcite/ *Corosex*^{TM} was obtained, then the column was operated under elevated Mn concentration (5 mg L^{-1} Mn^{2+}) with the chosen ratio to investigate the efficiency of the contactor in remineralization of soft water with simultaneous Mn removal. The column demonstrated high efficiency: in the long-term operation, the contactor was able to remove over 99% of dissolved Mn from the synthetic feed water (SFW) and added above 40 mg $CaCO_3$/L of hardness to the soft feed. The stable condition was reached much sooner than the previous phase when only calcite was used (10 h of operation versus above 100 h of operation). Accumulation of newly formed Mn residue increased the head loss overtime and caused filter clogging. It is important to note that using a blend of calcite and *Corosex*^{TM} does not seem like a promising option for long-term operation if the Mn concentration in the feed is unrealistically high (i.e. 5 mg L^{-1} Mn^{2+}). However, for more realistic Mn concentrations (i.e. 0.2 mg/L and less), adding a small portion of MgO to the filter would help to improve the hardness addition.

TABLE OF CONTENTS

LIST OF TABLES

LIST OF FIGURES

LIST OF SYMBOLS AND ABBREVIATIONS

AFM	Atomic Force Microscopy
BE	Binding Energy
BET	Brunauer–Emmett–Teller
Ca	Calcium
CCM	Constant Capacitance Model
DLM	Diffuse Layer Model
EBCT	Empty Bed Contact Time
EDTA	Ethylenediaminetetraacetic Acid
EDX	Energy Dispersive X-ray
FEG-SEM	Field Emission Gun Electron Microscope
GW	Groundwater
HFNF	Hollow Fiber Nanofiltration
ICP	Inductively Coupled Plasma
ICP-AES	Inductively Coupled Plasma - Atomic Emission Spectroscopy
ICP-OES	Inductively Coupled Plasma - Optical Emission Spectrometry
IX	Ion Exchange
LSI	Langelier Saturation Index
MGD	Million Gallons Per Day
Mn	Manganese
POE	Point of Entry
PWP	Plummer, Parkhurst, Wigley
SCM	Surface Complexation Model
SEM	Scanning Electron Microscope

SFW	Synthetic Feed Water
SMCL	Secondary Maximum Contaminant Level
SPM	Surface Precipitation Model
TLM	Triple Layer Model
USEPA	United States Environmental Protection Agency
XPS	X-Ray Photoelectron Spectroscopy

LIST OF APPENDICES

Chapter 1 **INTRODUCTION**

1.1 Background

Groundwater (GW) accounts for 96% of all unfrozen fresh water supply and provides nearly half of the world's drinking water supply. In North America, approximately 27% of Canadians and 44% of the United States population, mainly living in rural areas, rely on GW as their primary water supply. High manganese (Mn) concentrations often naturally exist in GW (Civardi & Tompeck, 2015). Apart from the fact that the presence of Mn in finished water causes aesthetic and operational issues, manganese is also under review in Canada and the US for a possible health-based regulation given the increased evidence of the neurotoxicity of manganese, especially for children (Bouchard et al., 2011; Dion et al., 2018). Thus, efficient removal of Mn from drinking water is an emerging concern. Catalytic filtration or cationic ion exchange (IX) coupled with point-of-use reverse osmosis are the processes most widely implemented to remove Mn and Fe from GW in domestic applications. However, the risk of Mn leaching from improperly operated point-of-entry catalytic filters, high salt consumption for IX regeneration and a considerable amount of brine waste production, which pollutes the environment, are common drawbacks of these treatment options. As an alternative, recently, Haddad et al. (2018) proposed the application of a hollow fiber nanofiltration (HFNF) membrane process for treating domestic GW supplies in small/remote communities or even for domestic applications where the financial and technical resources are important concerns. Even though the application of HFNF process can be an appealing solution for effective removal of Mn, Fe and pathogens, the non-selective property of the HFNF membranes may result in the almost complete depletion of GW hardness and alkalinity levels which would subsequently lead to the distribution of corrosive treated water. Therefore, the HFNF process should be coupled with a remineralization step (Haddad et al., 2018). To achieve this goal, filtration through a bed made of a blend of calcite (i.e., calcium carbonate), often mixed with magnesium oxide, is used as a remineralization strategy for domestic purposes and small water systems. This treatment option is most often referred to as calcite or limestone contactor. Remineralization of finished water from desalination plants is another common application of this process. Calcite dissolution adds calcium hardness and bicarbonate alkalinity which are two essential drinking water elements required to minimize water corrosivity. In this regard, several pieces of research have shown that calcite filtration is a reliable remineralization method as no continuous chemical addition is required and limestone is inexpensive, readily available, safe and easy to store and manipulate (Shemer et al., 2013; Van Der Laan. H., 2016).

Moreover, another interesting advantage of calcite lies in its ability to sorb divalent metallic cations (Me^{2+}) on its surface (Aziz & Smith, 1996; Franklin & Morse, 1983). Due to its high removal efficiency, a number of researchers recommended using calcite media for manganese removal from acid mine drainage (Aziz & Smith, 1992, 1996; Thornton, 1995; Zachara et al., 1991). As mentioned earlier, in drinking water applications, manganese removal is a common treatment

objective because of the fact that manganese naturally occurs in surface and groundwater supplies due to weathering and leaching of metal-bearing minerals, rocks and soils rich in organic matter, thermal stratification in lakes and contamination by industrial effluents (Kenari, 2017). It is anticipated that limestone contactor can be used to simultaneously remineralize soft waters as well as remove manganese. In this regard, the present investigation is a complement to the previous work of (Haddad et al. 2018) on designing a simple, yet robust system to efficiently treat domestic GW supplies.

1.2 Structure of the thesis

This thesis is divided into seven chapters. Chapter 1 presents a general background on corrosion control and Manganese removal. Chapter 2 presents a comprehensive literature review of the application of calcite contactors for remineralization and manganese removal in water treatment sector. The research objectives, hypotheses and methodology to carry out the specific objectives are presented in chapter 3. Chapter 4 presents results of this research in the form of a submitted manuscript to *Water Research Journal* followed by chapter 5 which mainly presents the supplementary results. The article intends to determine the effect of Mn-coating on calcite dissolution rate and eventually modeling the long-term behavior of a calcite contactor operated for drinking water remineralization. Finally, a general discussion is provided in chapter 6 followed by conclusions and recommendations.

Chapter 2 **LITERATURE REVIEW**

The literature review chapter is divided into two sections. The first section addresses the issue of remineralization via calcite contactor, and the second section discusses the literature assessing the performance of limestone contactor for Mn removal.

2.1 Remineralization

Remineralization process is considered for situations where it is needed to increase the mineral content of soft or demineralized water. Some surface waters are naturally soft, but the major source of demineralized water is the product of desalination plants. Purified bottled water is another area where increasing the mineral content of water is sought in order to improve the taste of water. Demineralized water is devoid of essential minerals, i.e., calcium and magnesium. This lack of minerals raises some problems such as corrosion in the pipelines, health impacts as well as poor organoleptic characteristics. Since soft water is highly reactive with metals, it can cause severe corrosion difficulties when it is transported through conventional pipelines (Shemer et al., 2012). On the other hand, it is also desirable to remineralize waters to meet health requirements because calcium and magnesium are necessary for normal metabolism in the body. The lack of these ions in demineralized water gives rise to health impacts of drinking soft water, including sudden cardiac death (Kozisek, 2004). However, there is currently no minimal hardness concentration required in Canadian tap waters. Nevertheless, untreated soft waters should not be used directly as a drinking water and a certain degree of remineralization is crucial to increase the buffering capacity and pH, also to mitigate corrosion by-products, such as copper, and reduce corrosion in the distribution system and more importantly to re-introduce some essential ions from a health perspective (Shemer et al., 2013; Shemer et al., 2012).

2.1.1 Remineralization options

There are several options for remineralization but the primary objective of a remineralization process is to increase the Langelier Saturation Index (LSI) and increase the bicarbonate alkalinity and pH value of the targeted water (Withers, 2005). In the water industry, remineralization is generally achieved by the following three methods (Withers, 2005):

- Chemical solutions dosing (based on calcium chloride and sodium bicarbonate)
- Carbon dioxide addition followed by lime dosing; or
- Carbon dioxide addition followed by calcite contactor.

Lime and caustic soda dosing can also be employed to readjust the pH. However, they typically provide only a small increase in alkalinity and hardness. As both chemicals are strong bases, low dosages are needed to increase pH to a target value typically ranging from 7.5 to 8.3. For such small dosages, the increase in mineral content is moderate to low. Nevertheless, these two options

are extremely common given that they are cost-effective in larger municipal systems. Various corrosion inhibitors are also used in the municipal water treatment sector (Withers, 2005). However, all the techniques mentioned above are implemented at municipal scale, for domestic purposes and small water systems, filtration through a bed made of a blend of calcite (i.e., calcium carbonate), often mixed with magnesium oxide (MgO), is often used as a remineralization strategy, which is referred to as calcite or limestone contactor. The main reason for adding MgO to the calcite media is due to the documented health benefits of Mg intake on cardiac health ((WHO), 2011). Remineralization of finished water from desalination plants is another common application of this process. As the primary goal of this study is to design a simple, yet robust system for efficient treatment of domestic GW supplies, calcite contactor is the best option for such a purpose as no continuous chemical addition is needed and limestone, as mentioned earlier, is inexpensive, readily available, safe and easy to store and manipulate (Shemer et al., 2013; Van Der Laan. H., 2016).

2.1.2 Calcite contactor process for remineralization

Calcite contactor is a filtration technique in which water passes through a bed of calcite grains while dissolving carbonate minerals from the grains into the passing water until the pH approaches equilibrium with calcium carbonate. Alkalinity, calcium, pH, and dissolved inorganic carbon concentrations increase with calcite dissolution (Yamauchi et al., 1987). The main components of a calcite bed include a contact tank which is filled with calcite grains, influent and effluent line, overflow line and access lid (mainly for media refill). Figure 2-1 is a schematic illustration of a typical calcite contactor. Equilibrium conditions depend on the contact time and initial water characteristics (pH, CO_2 content, calcium, alkalinity and temperature) (Yamauchi et al., 1987). The calcium concentration of the feed water approaches that of the equilibrium but cannot exceed it (approx. 45-50 mg $CaCO_3$/L). Calcite grains should be periodically added to the bed to replace dissolved media.

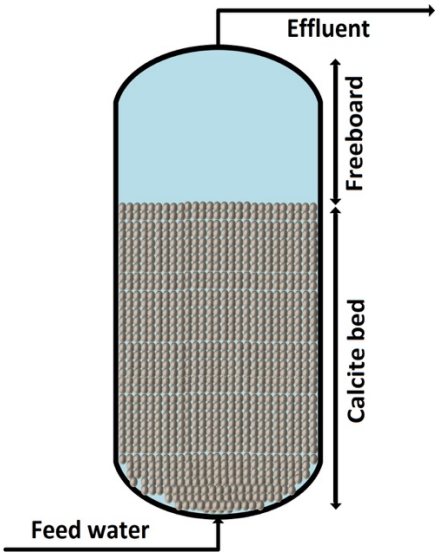

Figure 2-1: Schematic of a calcite contactor

2.1.3 Theory of Calcite dissolution

When water flows through a fixed bed of calcite grains, calcite dissolves which causes an enrichment in calcium ions and carbonate alkalinity. The parallel chemical reactions illustrating calcium carbonate equilibrium at 10 °C that is taking place in the solid/water interface are described below through Eqs. 2.1 to 2.5 (Lehmann et al., 2013).

$CaCO_3 \leftrightarrow Ca^{2+} + CO_3^{2-}$ $K_s = [Ca^{2+}] * [CO_3^{2-}] = 4.4*10^{-9}$ $pk_s = -8.36$ 2-1

$CO_2 + H_2O \leftrightarrow HCO_3^- + H^+$ $K_1 = \frac{[HCO_3^-]*[H_3O^+]}{[CO_2]} = 3.44*10^{-7}$ $pk_1 = -6.46$ 2-2

$HCO_3^- + H_2O \leftrightarrow CO_3^{2-} + H_3O^+$ $K_2 = \frac{[CO_3^{2-}]*[H_3O^+]}{[HCO_3^-]} = 3.25*10^{-11}$ $pk_2 = -10.49$ 2-3

$CaCO_3 + CO_2 + H_2O \leftrightarrow Ca^{2+} + 2HCO_3^-$ $K_a = \frac{[Ca^{2+}]*[HCO_3^-]^2}{[CO_2]} = 4.6*10^{-5}$ $pk_a = -4.33$ 2-4

$$[Ca^{2+}] = {}^1/_2\,[HCO_3^-] \quad 2\text{-}5$$

Where:

$K_{1, 2, a}$ = reaction constant at 10°C (mole/m^2/s)

K_s = solubility product of calcite

pk = - log(k)

[] = stoichiometric molar concentration (mol/l).

2.1.4 The reaction rate of calcite dissolution

The reaction rate is the speed at which a reaction occurs. In the dissolution of solids in water, the reaction rate can be calculated by either dissolution kinetics or mass balance. A general dissolution kinetic can be expressed using Eq. 2-6 which can be simply written for calcite grains:

$$\frac{dM}{dt} = k * A \qquad 2\text{-}6$$

Where:

dt = contact time (s)

k = rate constant of calcite dissolution (mole/m^2/s)

A = surface area of calcite grains (m^2)

On the other hand, based on the principle of mass conservation, the mass change in the solid should be equal to that of the liquid phase (Fogler, 1999):

$$\mathrm{dM} = \mathrm{dC} * \mathrm{V} \qquad 2\text{-}7$$

Where:

dM = mass change (mol)

dC = concentration change (mole/m^3)

V = volume of the reactor (m^3)

Finally, calcite dissolution rate can be written as follows:

$$\frac{dC}{dt} = k * \frac{A}{V} \qquad 2\text{-}8$$

As it is seen from the above equation, $\frac{A}{V}$ (surface to volume ratio) plays an important role in the calcite dissolution rate. This ratio can be calculated for different shapes by the following equation:

$$\frac{A}{V} = \frac{6*(1-\varepsilon)}{d*\varphi} \qquad 2\text{-}9$$

Where:

d = diameter of the grain (m)

ε = porosity of the filter bed

φ = shape factor

$$\varphi = \frac{\frac{A_{sphere}}{V}}{\frac{A_{irregular}}{V}} \quad 2\text{-}10$$

2.1.5 Calcite dissolution models

The three most common calcite dissolution models are the ones of Plummer, Parkhurst, Wigley (PWP) (1978), Yamauchi (1987) and Letterman (1987) (Letterman et al., 1987; Plummer et al., 1979; Plummer et al., 1978; Yamauchi et al., 1987). In the PWP and Yamauchi models, it is assumed that the flow is turbulent and the process is very fast; thereby, the calcite dissolution is controlled only by surface reactions, i.e., diffusional mass transport is neglected (Ghanbari, 2018; Plummer et al., 1979; Yamauchi et al., 1987). On the other hand, in the Letterman model, mass transfer is the key controlling mechanism used to predict calcite dissolution (Letterman et al., 1987).

Table 2-1: Major features of the calcite dissolution models

Model	System description	Assumptions
Plummer et al. (PWP) (Plummer et al., 1979)	Dissolution of 0.3-0.6 mm calcite grains in a stirred system at temperatures of 5-60°C opened to atmospheric CO_2 (in contact with a constant pressure of CO_2)	- Diffusional mass transfer is neglected - Concentration of aggressive CO_2 is used as the driving force - Dissolution occurs by the three simultaneous chemical reactions: $CaCO_3 + H^+ \Leftrightarrow Ca^{2+} + HCO_3^-$ (I) $CaCO_3 + H_2CO_3 \Leftrightarrow Ca^{2+} + 2HCO_3^-$ (II) $CaCO_3 + H_2O \Leftrightarrow Ca^{2+} + CO_3^{2-} + H_2O \Leftrightarrow$ $Ca^{2+} + HCO_3^- + OH^-$ (III)
Yamauchi (Yamauchi et al., 1987)	Dissolution of 1.4-10 mm calcite particles via a flow of CO_2 acidified distilled water at 40°C in a 100 mm diameter column with the following characteristics: Packing length = 0.5-2.4 m $[CO_2]_{feed}$ = 2.4-5 mM	- Diffusional mass transfer is neglected - The surface chemical reaction controls the dissolution reaction - Concentration of aggressive CO_2 is used as the driving force

	Retention time = 55-270 s Closed to atmospheric CO_2	- Calcite dissolution has no effect on the size of the calcite particles as they are replaced by fresh calcite frequently. - Ideal plug flow
Letterman (Letterman et al., 1987)	Dissolution of 9.6-32 mm calcite particles by a flow of HCl-acidified soft water between 9°C and 22 °C in four 150-380 mm diameter columns with the following characteristics: -Packing length = 2.1-3.5 m $[CO_2]_{feed}$ HCl acidity = 0.002-0.4 mM -Retention time = 230-3800 s - Closed to atmospheric CO_2	- Dissolution is assumed to be controlled by the use of three resistances in series: (1) liquid film transfer; (2) surface reaction; and (3) residual layer mass transfer. - The calcium difference is used as the driving force. - The calcite dissolution has no effect on the size of the calcite particles as they are replaced by fresh calcite frequently. - Non-ideal flow with dispersion effect

2.1.6 Parameters affecting the calcite dissolution rate (contactor design)

The rate of calcite dissolution and generally efficiency of a calcite contactor is highly dependent on various factors such as influent water composition, empty bed contact time (EBCT), media characteristics and superficial velocity (Shemer et al., 2013). In what follows, the effect of each parameter on the performance of a calcite contactor is discussed based on the relevant information from the literature.

2.1.6.1 Influent water characteristics

2.1.6.2 Impurities in the feed water

Past research has shown that calcite dissolution is adversely affected by the presence of substances like magnesium, organic matter and copper (Arvidson et al., 2006; Erga, 1956; Morse et al., 2007). (Arvidson et al., 2006), by surface observations using atomic force microscopy (AFM), have shown that calcite dissolution is decreased in the presence of dissolved magnesium. For the purpose of the present study, the impact of inhibitors will be neglected since the main focus of this research is remineralization of highly pure water derived from HFNF process, so investigating the adverse effects of inhibitors such as metallic impurities is beyond the scope of this research effort.

2.1.6.3 Saturation state of calcite

The driving force for calcite dissolution is its saturation state with respect to $CaCO_3$ and dissolution occurs only in a condition that the water is undersaturated with $CaCO_3$. The Langelier Saturation Index (LSI) is one of several tools used to estimate the degree of saturation of calcium carbonate in water (Ghanbari, 2018). The general formula to calculate the Langelier Saturation Index (LSI) is as follows (Benefield et al., 1982):

$$LSI = pH - pH_S \qquad 2\text{-}11$$

Where:

pH = measured pH of the sample

pH_s = calculated saturation pH of the same sample

And once it is calculated, one of the three following scenarios can happen (Benefield et al., 1982):

- LSI>0 Water is undersaturated with respect to calcium carbonate and will not accept more CaCO3.
- LSI=0 Water is neutral, so it is neither scale-forming nor scale removing.
- LSI<0 Water is undersaturated with respect to calcium carbonate and tends to dissolve more calcium carbonate.

2.1.7 Calcite media characteristics

(Ruggieri et al., 2008) conducted a research on limestone selection criteria and concluded that calcite dissolution rate could be enhanced or inhibited depending on available reaction surface area of grains and the impurities they contain. According to the general calcite dissolution rate formula (Eq. 2-8), the higher the specific surface area (A/V), the higher the calcite dissolution rate is, hence the lower the required EBCT to reach the equilibrium. Obviously, A/V ratio is affected by the size and/or sphericity of a grain. A number of researchers claimed that smaller calcite particles have a superior dissolution rate due to their larger specific surface area (Letterman et al., 1991; Shemer et al., 2013; Yamauchi et al., 1987). Based on a research carried out by (Hernández-Suárez, 2005), limestone bed height is influenced by the particle diameter, as shown in the Fig. 2-2. Finally, it is important to note that calcite size will progressively be reduced as the particle dissolves in water. Therefore, a calcite bed is expected to include media with variable particle size, a phenomenon which complexifies the modeling of calcite dissolution in packed bed reactor.

Based on a report published by Texas Water Treatment Board, the recommended height of the calcite contactor should be in the range of 1 to 3 meters (3 to 10 feet) (W. Walker, 2012).

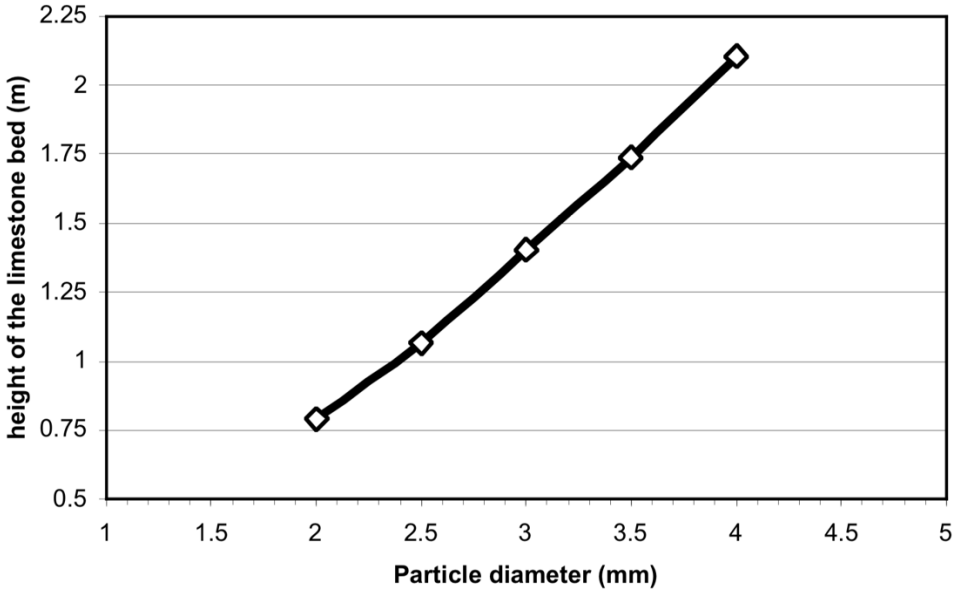

Figure 2-2: Example of a relationship between particle diameter and height of the limestone bed (Hernández-Suárez, 2005).

More recently, S. Ghanbari (2018) tabulated shape factor for different geometries using Eq. 2-10, as shown in table 2-2. According to the table, a spherically shaped grain has a smaller surface area than the irregularly shaped ones (Ghanbari, 2018).

Table 2-2: Shape factor for different shapes and their ratio compared to the standard spherical shape (volumes are kept the same)

Form	**Unites**	**V(mm^3)**	**a(mm)**	**A(mm^2)**	**A/V(mm)**	**Compare to spherical ($A/V/A_p/V_p$)**
Spherical	a	0,52	1,0	3,14	6	1,00
Rectangle	a, b = a/3 h =2a	0,52	0,9	5,11	10	1.66
Square	a	0,52	0,8	3,90	7	1.16

Tetrahedron	a	0,52	1,6	4,68	9	1.5
Cylinder	a, h = 2a	0,52	0,7	3,78	7	1.16
Cone	a, a=h	0,52	1,3	5,17	10	1.66

As mentioned earlier, calcite dissolution rate is also dependent upon the chemical characteristics like the amount and type of impurities. Ruggieri et al. (2008) carried out a research on limestone selection criteria for water remineralization and they used five different calcite samples containing a different percentage of impurities (Ruggieri et al., 2008). Table 2-3 demonstrates a summary of the composition of the calcite samples used.

Table 2-3: Characterization of limestone samples (L1 to L5)

Sample	**L1**	**L2**	**L3**	**L4**	**L5**
%$CaCO_3$ purity	98.3	97.9	99.6	92.8	97.5
% MgO	0.20	0.35	0.36	3.26	0.55
% Al_2O_3	0.04	0.25	0.02	0.15	0.43
% Fe_2O_3	0.03	0.12	0.01	0.25	0.26
Particle size (μm)	<5	<20	<5	>100	>100
BET surface area (m^2/g)	0.43	0.66	0.11	0.26	0.82

Specific conductivity of the finished water was used as an indicator of limestone dissolution, as shown in Fig. 2-3. The authors observed textural differences between used calcite samples which can be reflected via physical properties of the samples (i.e., BET specific surface). Although samples had a different particle size, their cementing ability were different which resulted in different BET specific surface. Hence a solid conclusion cannot be made based on their results as to whether the impurity or particle size had the dominant influence on calcite dissolution rate.

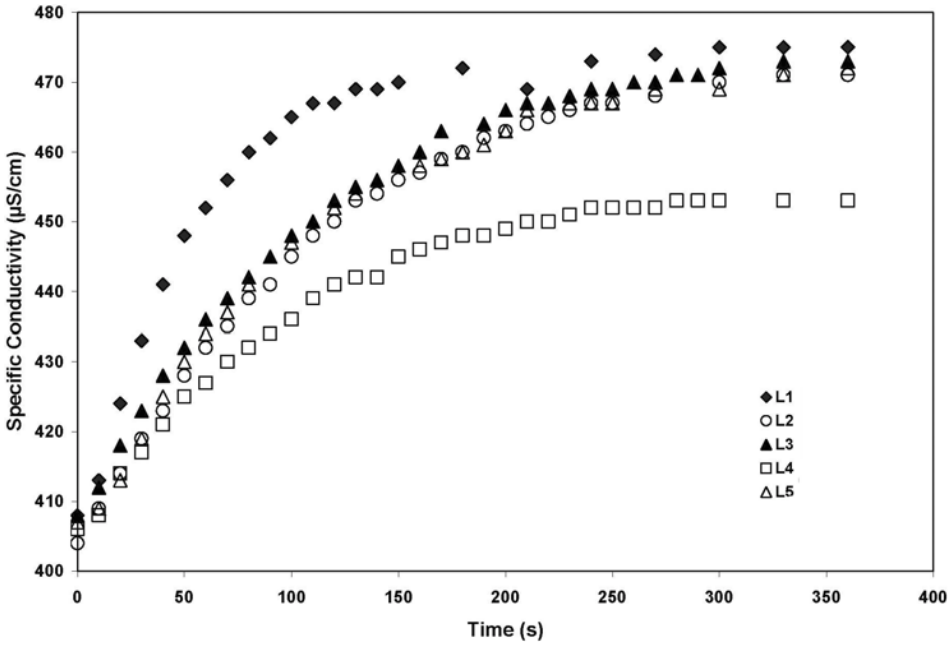

Figure 2-3: Specific conductivity of the finished water VS. contact time achieved with different calcite samples (L1 to L5) (Ruggieri et al., 2008).

2.1.8 Empty Bed Contact Time (EBCT)

EBCT is a measure of the time that water is in contact with calcite media in the contactor, assuming that all liquid passes through an empty vessel at the same velocity. EBCT is equal to the empty filter bed volume divided by the flow rate which can be calculated using Eq. 2-12.

$$EBCT = \frac{volume\ of\ the\ filter\ bed}{flow\ rate} = \frac{V_B}{Q} \qquad 2\text{-}12$$

The EBCT can be adjusted by either manipulating the flow rate or taking samples from different heights throughout the bed. From a process control point of view, it is important that the reaction reaches the equilibrium before leaving the bed to achieve calcium carbonate saturation. In order to do so, the EBCT should be long enough and account for variation in daily flow as well as the progressive expected reduction in bed height due to calcite dissolution. (Ghanbari, 2018; Van Der Laan. H., 2016). The recommended EBCT for a calcite contactor for remineralization purposes ranges from 10 to 30 minutes (Bang, 2012; Ghanbari, 2018; Nikolay, 2012).

2.1.9 Superficial velocity or loading rate

Superficial velocity is representative of the hydrodynamic condition inside the contactor. It is also known as the loading rate which is defined as the flow rate divided by the cross-sectional area of the contactor. From a mass transfer point of view, augmenting the flow rate minimizes the boundary layer thickness. This affects film diffusion as a result of increased Reynolds number, which will result in augmenting the mass flux between the bulk solution and the solid surface

(increasing reaction rate) (Lehmann et al., 2013). According to a research conducted by (Lehmann et al., 2013) on design aspects of calcite contactors applied for post-treatment of desalinated water, increasing the superficial velocity tends to increase the dissolution rate, as shown in Fig. 2-4 (Lehmann et al., 2013). However, it is worth noting that increasing the superficial velocity should not be an objective because the required EBCT to reach equilibrium, also known as design EBCT, is inversely related to the superficial velocity. As can be seen on Fig. 2-4, the improved mass transfer achieved at higher velocity is not significant. Thereby, a higher velocity needs a higher bed height so that the design EBCT is kept constant which is not advantageous from a process design point of view.

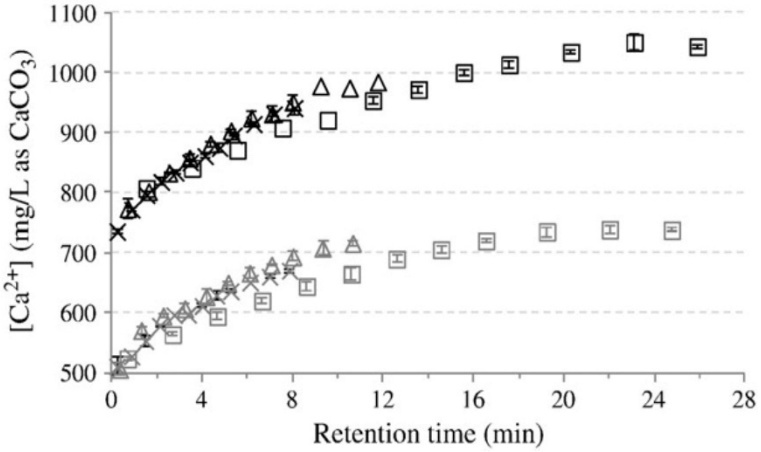

Figure 2-4: Average $[Ca^{2+}]$ in the calcite reactor as a function of retention time for the six case studies: 10, 20, and 30 m/h flow rates (□, Δ, and X, respectively) and gray and black signs for the 2 different acid dosages of 490 and 721 mg H_2SO_4/L (Lehmann et al., 2013).

The Texas Water Treatment Board published a report on up-flow calcite contactor design in which they reported the design superficial velocities of calcite contactors for several different case studies. Table 2-3 is a summary of design superficial velocities and the particle size used in these studies (W. Walker, 2012). It is important to note that fine particles from calcite beds, which are dragged upstream, can influence the turbidity of the effluent which is a source of concern in drinking water treatment industry. Accordingly, if too many fines (< 80 micrometer) are present in the calcite media, turbidity is a source of concern because the relationship between superficial velocity and turbidity is highly dependent on the quality of the calcite. Figure 2.5. shows the relationship between turbidity and superficial velocities for calcite with two different kind of media consisting of less than 1 percent fines and with 2-3 percent fines. For the first sample (less than one percent of fines), turbidity starts to increase at around 15 meters per hour (m/hr) and for the second sample with 2-3 percent fines, turbidity starts to increase at around 11-12 m/h.

Table 2-3: Design superficial velocities and particle size used for calcite contactors in different case studies (Walker, 2012).

Reference site	Plant size (MGD)	Superficial velocity (ft/min)	Calcite particle size (mm)
Alicante II, Spain	18	0.48	1-3
Barcelona, Spain	53	0.67	1-3
Blue Hills, Bahamas	3.6	0.56	1
Stellenbosch, South Africa	38	0.55	11-14
Mars Hill, Maine	0.3	0.13	25

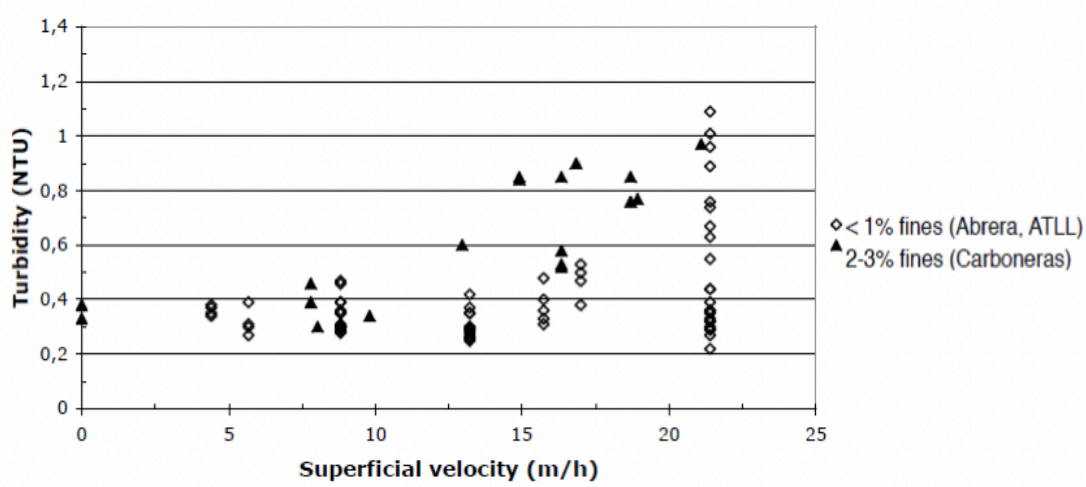

Figure 2-5-Relationship between superficial velocity (m/h) and turbidity

As a brief conclusion based on the cited literature remark on the calcite dissolution rate, the dissolution is favored by:

- Lower feed water pH (increasing the CO_2 concentration)
- Smaller particle size
- Higher EBCT
- Lower temperature
- Lower particle sphericity
- Higher superficial velocity

2.2 Manganese removal

Manganese (Mn) is one of the emerging contaminants abundantly present in many water sources (Aziz & Smith, 1996; Franklin & Morse, 1983). In drinking water applications, manganese removal is a common treatment objective. The occurrence of manganese in drinking water gives rise to aesthetic and operational issues which increases the cost of cleaning or renewing fouled pipes (Tobiason et al., 2016). In addition, manganese is under review in Canada and the US for a possible health-based regulation given the increased evidence of its neurotoxicity, especially marked intellectual impairment in school-age children (Bouchard et al., 2011; Dion et al., 2018). Thus, efficient removal of Mn from drinking water is crucial. The United States Environmental Protection Agency (USEPA) (USEPA, 2004) has regulated the Secondary Maximum Contaminant Level (SMCL) of 0.05 mg/L for total manganese in drinking water. However, consumer complaints concerning aesthetic issues have been reported at concentrations as low as 0.02 mg/L (Sly et al., 1990). Consequently, Health Canada (Health-Canada, 2016) has recently proposed an aesthetic objective limit of 0.02 mg/L for total manganese in drinking water and 0.1 mg/L for health-based purposes. Therefore, it is recommended to keep the level of these minerals in drinking water as low as possible (Kenari, 2017).

2.2.1 Manganese removal options

Mn removal from drinking water sources can be carried out by different methods (Tobiason et al., 2016). A common treatment technique for Mn removal, applied in the municipal water treatment sector, is oxidation by a strong chemical (e.g. $KMnO_4$) followed by precipitation and particle removal (Kothari, 1988). As on-line chemical injection is challenging in small-scale applications, point-of-entry (POE) catalytic filtration with intermittent regeneration or POE cationic ion exchange (IX) coupled with point-of-use reverse osmosis are two widely implemented options to remove Mn in domestic applications (Carrière et al., 2011). However, the risk of Mn leaching from improperly operated catalytic filters, the high salt consumption for IX regeneration and the considerable amount of brine waste production, which pollutes the environment, are common drawbacks of these methods (Barbeau et al., 2011; Carrière et al., 2011).

Mn can also be removed from solution by sorption to a solid surface, manganese oxide ($MnO_{x(s)}$) is the most often used media for Mn removal (Silva et al., 2012; Tobiason et al., 2016). As an alternative, recently, Haddad et al. (2018) proposed the use of back-washable hollow fiber nanofiltration (HFNF) membranes for the removal of Mn and Fe from groundwater (Haddad et al., 2018). The authors concluded that even though the application of the HFNF process could be an appealing solution for effective removal of Mn and Fe, non-selective rejection properties of the HFNF membrane would result in a corrosive permeate water. Therefore, the HFNF process should be coupled with a polishing step to adjust the hardness level of its soft permeate (Haddad et al., 2018). It should be noted that another interesting advantage of calcite lies in its ability to sorb divalent metallic cations (Me^{2+}) on its surface (Aziz & Smith, 1996; Franklin & Morse, 1983). Due to its superior efficiency, a number of researchers recommended using calcite media for manganese

removal from acid mine drainage (Aziz & Smith, 1992, 1996; Thornton, 1995; Zachara et al., 1991). It has also shown a greater efficiency over other media such as brick powder and gravel (Aziz & Smith, 1992, 1996; Thornton, 1995; Zachara et al., 1991). Therefore, calcite contactor could be a final polishing step for HFNF process to further reduce dissolved manganese which was not necessarily entirely rejected by the HFNF membrane process (Haddad et al., 2018). To achieve very high rejection of Mn with NF, one must select membranes with very low molecular weight cut-offs (<100 Da), a decision which imposes higher pressure of operation and/or lower productivity. The use of a limestone contactor after NF could offer the advantage of changing the selection of the NF membrane to more porous ones.

2.2.2 Sorption of manganese on calcite surface

Calcite-Mn interaction and particularly the fate of various phases in the complex system of $CaCO_3$-$MnCO_3$-H_2O has been well documented in the literature (Franklin & Morse, 1983; Kothari, 1988; McBride, 1979; Pingitore et al., 1988; Silva et al., 2012; Thornton, 1995; Zachara et al., 1991). In 1979, McBride investigated the chemisorption of Mn^{2+} on calcite surface and proposed a reaction mechanism, as shown through Eqs. 2-13 to 2-15. The author suggested that the quantity of Ca ions released to the water is very similar to the quantity of Mn^{2+} adsorbed on the surface, but this phenomenon was not a direct displacement of ions, but rather the Mn^{2+} is sorbed on the surface as $MnCO_3$ which produces a proton that reacts with calcite to release Ca ions (McBride, 1979). Furthermore, since no adsorption maximum is determined in these studies, it can be deduced that both precipitation-adsorption were involved in the interaction between Mn and calcite (McBride, 1979).

$$Mn^{2+} + HCO_3^- \rightarrow MnCO_3 + H^+ \qquad 2\text{-}13$$

$$H^+ + CaCO_3 \rightarrow Ca^{2+} + HCO_3^- \qquad 2\text{-}14$$

The overall reaction mechanism proposed by McBride (1979) can be written as Eq. 2-15

$$Mn^{2+} + CaCO_3 \rightarrow MnCO_3 + Ca^{2+} \qquad 2\text{-}15$$

Apart from this, McBride also observed that Mn^{2+} adsorbed to the surface more than available adsorption sites, based on unit cell size and area measurement. This further supported his assumption that both precipitation-adsorption were involved (McBride, 1979). Another interesting conclusion of McBride's investigation was that at low Mn^{2+} concentrations (i.e., 0.1 mg Mn L^{-1}) at calcite surface, no discrete phase is formed but at higher concentrations, $MnCO_3$ nucleation occurs which is followed by a slow growth phase of $MnCO_3$ (McBride, 1979). In 1982, Franklin and Morse studied the interaction of Mn with the surface of calcite in dilute solutions and seawater. The authors concluded that Mn^{2+} is rapidly adsorbed to the surface, causing $MnCO_3$ nucleation which is followed by a growth phase of $MnCO_3$ by a first order reaction. However, in seawater which contains high concentrations of Mg^{2+}, the nucleation of $MnCO_3$ is inhibited because Mg^{2+} competes with Mn^{2+} on adsorption sites, preventing enough adsorption of Mn^{2+} on the surface to

reach a critical concentration of $MnCO_3$ nucleation (Franklin & Morse, 1983). In 2010, (Silva et al., 2010) studied the interaction of Mn^{2+} and calcite during mine water treatment. The authors claimed that the nucleation of the discrete phase of $MnCO_3$ takes place at the surface of the calcite media. By contrast, a number of researchers indicated that a dilute solid solution of Mn^{2+}-$CaCO_3$ is formed at the surface due to the displacement of Mn^{2+} in the calcite matrix (Comans & Middelburg, 1987; McBride, 1979; Pingitore et al., 1988). According to literature, the most commonly accepted kinetic for Mn and calcite interaction includes an initial rapid uptake of the trace metal (i.e., Mn) followed by a relatively slow formation of a solid solution expressed as $Mn(x)Ca(1-x)CO_3$; where composition (x) changes gradually between the original solid and precipitate of the sorbate which is gradually formed (Farley et al., 1985; McBride, 1979; Zachara et al., 1991). The initial rapid step is generally linked to an adsorption reaction while the following slow uptake is mainly attributed to the formation of solid solution and removal by precipitation at the surface. A number of researchers claimed that at low aqueous concentration (i.e., 0.1 mg Mn L^{-1}), metals only incorporate into the surface of calcite by adsorption with no solid solution formation (Comans & Middelburg, 1987; Franklin & Morse, 1983; McBride, 1979; Zachara et al., 1991). (Zachara et al., 1991) reported that metals with ionic radii smaller than Ca were more prone to sorb on calcite. Moreover, it should be noted that Mn^{2+} exhibits a very slow desorption rate which favors the application of calcite for Mn sorption in the water treatment field (McBride, 1979; Zachara et al., 1991).

According to Stumm and Morgan (1995), it is also possible to have other species in pH ranges 8-10 (Fig. 2-6). Although the possibility of $MnCO_3$ formation is higher than other species in the mentioned pH range, given the potential of feed water used in the above-mentioned studies (-0.5 - 0.5), the presence of oxides and hydroxides is also possible. However, characterization of filter media coating is crucial to better understand the driving force behind high efficiency of manganese removal in elevated Mn concentrations.

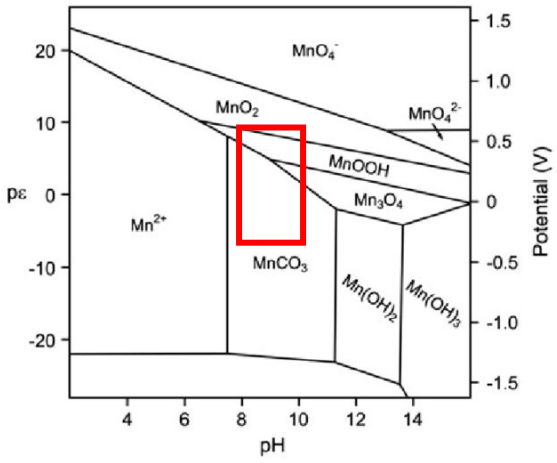

Figure 2-6: potential (E h in V) as a function of the pH showing the stability zones of manganese-containing compounds in aqueous solution. Source: adopted from Stumm and Morgan (1970)

2.2.3 Models describing Mn sorption on calcite surface

Modeling divalent metals sorption on carbonate minerals has received considerable attention over the last decades, including the modeling of Mn sorption on the surface of calcite (Comans & Middelburg, 1987; Farley et al., 1985). Surface precipitation model (SPM) and surface complexation model (SCM) are the two main modeling approaches used to describe the sorption of divalent metals on calcite. In the former model, it is considered that the precipitation on the solid is based on solid solution formation where the composition of the newly formed solid solution is continuously changing between that of the original solid and the precipitated sorbate layer (Farley et al., 1985; Mettler et al., 2009). (Comans & Middelburg, 1987) investigated the SPM model applicability to describe the sorption of divalent metals on calcite and proposed a continuum between adsorption and precipitation for Mn^{2+} sorption on calcite. According to (Zachara et al., 1991) findings, adsorption constants for different divalent metals in SPM are ranked based on the degree for which the ionic radius of the sorbate matches the ionic radius of Ca^{2+}. It is worth mentioning that SPM was also successfully applied for modeling Mn^{2+} sorption on siderite ($FeCO_3$) surface (Wersin et al., 1989). The Surface Complexation Model (SCM), on the other hand, is based on an initial rapid adsorption step followed by surface complexation prior to the precipitation of $MeCO_3$ and dilute solid solution formation. Three common versions of the SCM model have been used to describe metal ion adsorption on pure mineral materials: constant capacitance model (CCM), diffuse layer model (DLM), and triple layer model (TLM) (Wen et al., 1998).

2.3 Knowledge gap based on the literature review

Despite the fact that there are several comprehensive studies addressing both the implementation of calcite contactors in the water industry as a simple and reliable remineralization and corrosion control technique and Mn adsorption on the surface of calcite, the integration of both processes to a single stage process has not received enough attention. Furthermore, to the best of our knowledge, the significance and fate of sorbed Mn and its impact on the overall performance of a calcite contactor in a long-term operation has not been addressed yet. In this regard, the primary goal of this research effort is to determine the detrimental effect of Mn-coating on calcite dissolution rate and eventually model the long-term behavior of a calcite contactor operated for simultaneous drinking water remineralization and Mn removal. The outcome of this study would enable us to design a simple, yet robust system for an efficient treatment of domestic GW supplies.

Chapter 3 RESEARCH OBJECTIVES, HYPOTHESES AND METHODOLOGY

3.1 Objectives and hypotheses

3.1.1 General objective

The main objective of this research effort is to design a calcite contactor as a reliable and simple method for polishing the soft permeate of HFNF process. This polishing step will simultaneously remineralize the soft permeate and reduce dissolved manganese which was not necessarily entirely rejected by the HFNF process (target of 0.02 mg Mn/L and 40 mg $CaCO_3$/L as hardness in treated water).

3.1.2 Specific objectives

On a more detailed basis, the following specific objectives can be defined:

- Determine the role of the media specifications (i.e., use of pure calcite ($CaCO_3$) or a blend of calcite and *Corosex*^{TM} (MgO));
- Screen the best operational conditions for the efficient operation of a calcite contactor as a polishing step (i.e., temperature, EBCT, …);
- Investigate the significance and fate of sorbed Mn on the overall performance of a calcite contactor in long-term operation;
- Model the long-term behavior of a calcite contactor operated for drinking water remineralization.

3.1.3 Research hypotheses

- Mn sorption on calcite surface is reduced at lower temperature and higher EBCT;
- Mn coating on the calcite surface decreases the rate at which calcium carbonate dissolves into the water;
- A small portion of *Corosex*^{TM} media mixed with calcite can remineralize the water to above 40 mg $CaCO_3$/L while not disturbing the Mn removal process;

- A simple calcite dissolution rate based on calcite saturation index can be used to predict the long-term behavior of a calcite contactor with respect to calcite dissolution in the presence of manganese coating.

3.2 Methodology

The experimental approach was conducted in four main parts consisting of three experimental phases and one modeling phase:

1) In the first phase, the impact of initial Mn^{2+} concentration was investigated by means of continuous sorption-dissolution experiments. In this regard, we determined the overall performance of a calcite contactor in the removal of Mn and remineralization of SFW using two initial concentrations of Mn (i.e., 0.5 and 5 mg Mn L^{-1}).
2) Based on the results of the first phase, the objective of the second phase was to investigate the effect of Mn loading on calcite dissolution rate using continuous dissolution experiments. To this end, we transferred the loaded media from the loaded column used for the first phase to four mini-columns and operated them for five days in a continuous mode.
3) As for the third phase, the long-term efficiency of a calcite contactor was modeled based on calcite dissolution and Mn sorption/precipitation. The model was implemented in PHREEQC and it was used to investigate the long-term efficiency of a calcite contactor.
4) In the final phase, as we were not able to obtain the sought treated water characteristics with only calcite media, a blend of calcite (i.e., calcium carbonate), mixed with magnesium oxide (MgO) was used to achieve both goals of remineralization and partial Mn removal.

In what follows, the experimental protocol for each part is elaborated upon:

3.2.1 Continuous sorption-dissolution experiments with calcite media

3.2.1.1 Characteristics of synthetic feedwater (SFW) and calcite media

Synthetic feed water (SFW) was prepared by dissolving powdered reagent grade (>99% pure) $MnSO_4$ (Fisher Scientific, NJ, USA) in ultra-pure (i.e., Milli-Q™) water. Commercially available calcite (2.68 g/cm^3) media was purchased from Imerys Marble Inc, Sahuarita, AZ, USA. To determine the particle size distribution and accordingly the representative diameter of the grains, sieving analysis was executed on calcite media. The Fig. 3.1. demonstrates the results of sieving analysis and based on the results, the median diameter (D_{50}) of 0.40 mm was chosen as the representative diameter for future calculations. As the calcite grains were highly homogeneous, the D_{50} value is equal to average diameter of the grains (D_{10}) reported by Imerys Marble Inc, Sahuarita, AZ, USA. The main characteristics of calcite media are summarized in Table 3.1.

Table 3-1: Calcite media characteristics

Filter media	**D_{50} (1) (mm)**	**Purity (2) (%)**	**Specific gravity (3) (g/cm^3)**	**Bulk density (3) (kg/m^3)**	**Porosity (3) (ε)**	**Surface area (4) (m^2/g)**	**Other impurities (3)**
Calcite ($CaCO_3$)	0.4	99.70	2.68	1500	0.42	0.371	0.3 % Mg

(1) Measured in the laboratory using sieving
(2) Determined by Inductively Coupled Plasma-Optical Emission Spectrometry (ICP-OES, model iCAP 6000, Thermo Instruments Inc) after nitric acid acidification
(3) Provided by the supplier (Imerys Marble Inc, Sahuarita, AZ, USA)
(4) Data provided via BET measurement (The BET procedure is described in (Gambou-Bosca & Bélanger, 2016))

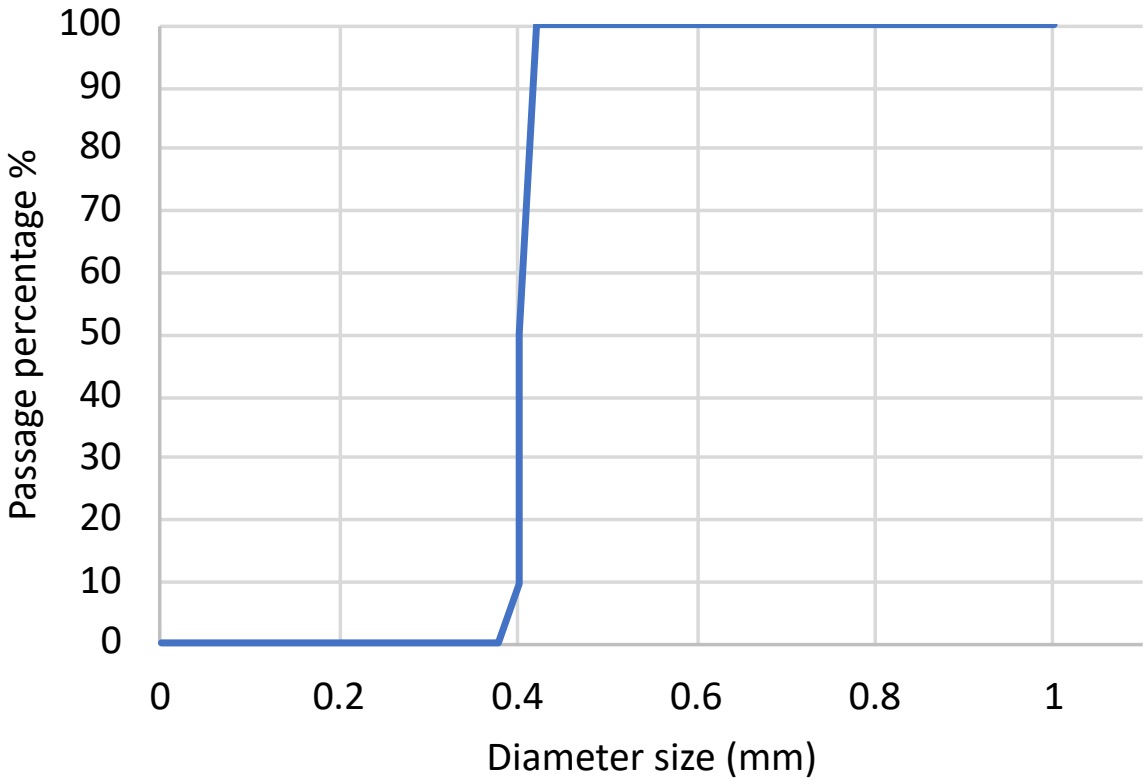

Figure 3-1: The size distribution curve for grain size ranging between 0.2-0.7

3.2.1.2 Experimental set-up and procedure

In Phase 1, sorption-dissolution experiments were conducted on calcite media in order to assess the efficiency of a calcite contactor for both remineralization and partial Mn removal. The assays were carried out at room temperature (i.e. 23 ± 2 °C) in two parallel cylindrical acrylic columns (1.3 m height and 31.75 mm internal diameter) filled to a height of 80 cm with fresh calcite media and continuously fed with SFW containing 0.5 mg Mn L^{-1} (column A) or 5 mg Mn L^{-1} (column B), respectively. The flow rate was set at 31.5 ml/min which translates into empty bed contact time (EBCT)=10 min in the second valve (at height of 40 cm) and 20 min in the effluent. It should be noted that these concentrations represent either high or very high Mn conditions in groundwater supplies (Health-Canada, 2016). The column-to-particle diameter ratio was approximately 79, which is considered sufficient to minimize wall effects. A schematic illustration of the sorption-dissolution set-up is shown in Fig. 3.2. Throughout the sorption-dissolution assays, samples were collected from four sampling points located at different heights and therefore representing increasing EBCTs. Samples were analyzed to determine Mn^{2+} concentration, pH and hardness, immediately after their collection. Hardness was measured by titration (Standard methods, Hardness (2340)/EDTA Titrimetric Method) while acidified manganese samples were analyzed by ICP-AES (Thermo-Fisher, ICAP 6000). Details of the ICP sample preparation and the applied measurement procedure can be found elsewhere (Haddad et al., 2018).

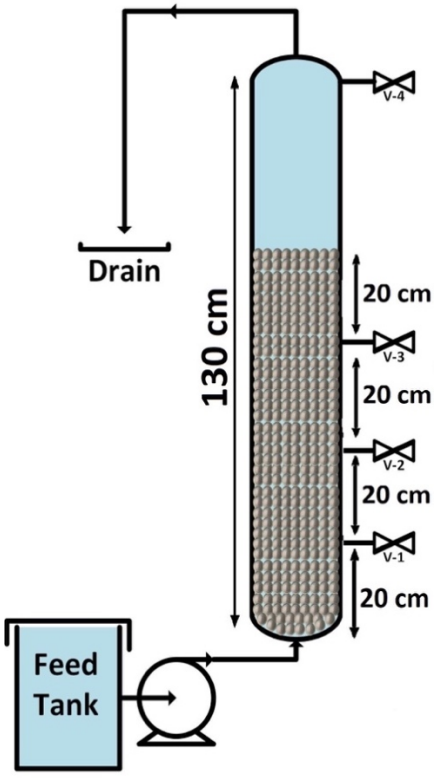

Figure 3-2: Schematic illustration of continuous sorption-dissolution set-up

3.2.1.3 Continuous desorption experiment

In order to investigate the Mn desorption rate, column B was fed with ultrapure water for 120 hours and samples were collected from two sampling points located at different heights and therefore representing increasing empty bed contact times. Samples were analyzed to determine Mn^{2+} concentration by ICP-AES (Thermo-Fisher, ICAP 6000).

3.2.1.4 Characterization of Mn-loaded calcite media

After long-term operation (800 hours) of sorption-dissolution columns (A and B), Mn-loaded calcite media samples were collected from different depths of the column B for further analysis using Scanning Electron Microscope (SEM), Energy Dispersive X-ray Analysis (EDX) and X-ray Photoelectron Spectroscopy (XPS) in order to characterize the media before and after loading and to determine the nature of the deposits found over the surface (Detailed description of each of these analyses are provided in the appendix A). This was done only for column B because a significant change in the color of the filter media was observed only for column B. To determine the quantity of Mn loaded on calcite, 160 mg of pre-weighted dried weights (with different Mn content) of media were digested in 15 mL of 10% (wt) HNO_3. Following complete dissolution, Mn concentrations were measured using ICP-AES.

3.2.2 Impact of Mn coating on calcite dissolution

3.2.2.1 Experimental set-up and procedure

The impact of Mn loading on calcite dissolution and Mn sorption was tested by transferring the Mn-loaded media from sorption-dissolution experiments to four mini-columns (20 cm media height and 1.5 cm internal diameter) with increasing Mn loadings ranging from 0 to 15 mg Mn/g of media (Table 3-2). A schematic of the mini-columns setup is shown in Figure 3.3. The experimental setup consisted of 5 mini-columns 4 of which were filled with Mn loaded calcite media with different Mn loading and the first column included fresh calcite media as a reference. The columns were fed with ultra-pure (i.e., Milli-Q™) water for 72 hours. Samples were frequently taken from the influent/effluents and characterized for Mn^{2+} content, hardness level and pH according to the methods described previously.

Table 3-2: Mn loading in the different mini-columns

# Columns	Column 1*	Column 2	Column 3	Column 4	Column 5
Mn content of the media (mg Mn^{2+}/g media)	0	1.06	2.13	4.02	14.97

* The control column with fresh calcite media

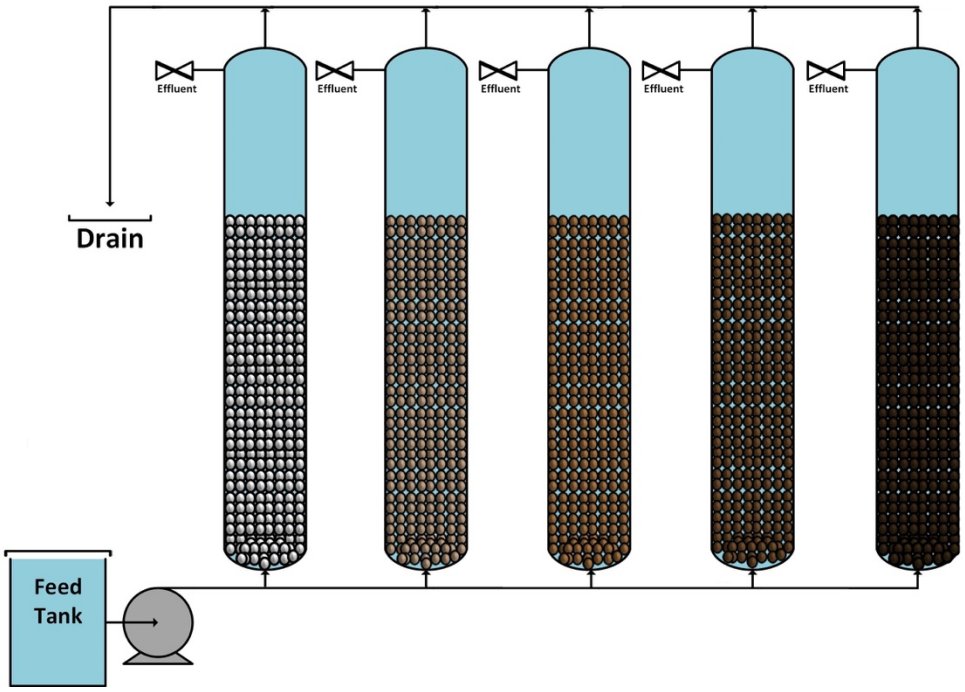

Figure 3-3: Schematic of mini-columns set-up

3.2.2.2 Batch sorption experiments on Mn-loaded media

True batch experiments were carried out at T =23°C to study the effect of Mn loading on calcite dissolution to investigate the ability of highly Mn-loaded calcite (collected from the bottom of the large column) in further removing Mn^{2+}. The sorption studies were performed by adding 10 g L^{-1} of Mn-loaded media to 200 mL flasks with various Mn^{+2} concentrations (0.0, 0.1, 1.0 and 10 mg Mn^{2+} L^{-1}). Throughout the sorption assays, the flasks were shaken (using Max Q2508 Thermo-Fisher shaker) at 150 rpm. At predetermined contact times (15 min, 1 h, 12h, 24 h, 48 h and 7d), a flask from each Mn concentration was removed, settled for 1-min and the supernatant was filtered using a 0.45 μm membrane filter (Supor ®PES Membrane Disc Filters, Pall, US) prior to Mn, hardness and pH measurements.

3.2.3 Model description and numerical simulations

The applied model in this study consisted of the equations for calcite dissolution, $MnCO_3$ formation (by ionic exchange between Ca^{2+} and Mn^{2+}) as well as the slow recrystallization of $MnCO_3$ into MnO_2 as indicated in Table 3-3. In this regard, a simple calcite dissolution rate based on calcite saturation index was defined. In (Claveau-Mallet et al., 2017), the successful application of the selected rate is reported for phosphorus precipitation in granular reactors. The calcite equilibrium constant was set at $pK_{spCAL} = 8.48$ according to standard geochemical database for crystalline calcite (Parkhurst & Appelo, 1999). The formation of MnO_2 was assumed according to mineralogical observations performed in this study (presented in the result section). The $MnCO_3$

precipitation rate was set as a first order reaction without $MnCO_3$ saturation assuming that autocatalytic sorption took place onto previously formed seeds. The $MnCO_3$ precipitation kinetic constant was increasing gradually to account for the increase of seeds. A saturation term of 1.8×10^{-7} M (10 μg Mn L^{-1}) was included in the rate to represent the lowest residual concentration observed in the effluent of the calcite contactor.

Calcite dissolution was presumed to be progressively limited by the formation of a thin MnO_2 film over the calcite grains. The diffusion of Ca^{2+} and CO_3^{2-} ions through the film was modelled based on Fick's law. At each iteration step, both dissolution and diffusion rates were calculated, and only the smallest rate was applied (which resulted in dissolution control at first and diffusion control afterward).

Table 3-3: Applied equations for calcite dissolution and manganese removal modeling

Processes	Stoichiometry					Rate law
	Ca^{2+}	CO_3^{2-}	Mn^{2+}	H^+	e^-	
Calcite dissolution	-1	-1				$r_{CAL} = k_{CAL} log\left(\frac{\{Ca^{2+}\}\{CO_3^{2-}\}}{K_{spCAL}}\right)$
Calcite diffusion through MnO_2 thin film	-1	-1				$r_{diff} = \frac{0.001 D_{barr}\left(K_{spCAL} - \{Ca^{2+}\}\{CO_3^{2-}\}\right)}{d_{barr}}\left(\frac{S0.001(1-n)}{n}\right)$
$MnCO_3$ formation by ionic exchange from calcite matrix	+1		-1			$r_{MnCO3} = k_{MnCO3}([Mn^{2+}] - 1.8 \times 10^{-7})$ $k_{MnCO3} = 10^{(A * X_{Mn} - B)}$ Note: 1.8×10^{-7} is a saturation term describing the min concentration of Mn^{+2} (based on experimental measurements)
Recrystallization of $MnCO_3$ into MnO_2		+1		+4	+2	$r_{MnO2} = k_{MnO2}([MnCO_3] - [MnO_2])$

X_{Mn}: total Mn precipitated in the calcite contactor (mol/L void volume); A and B: constants for seeding; D_{barr}: diffusion coefficient in the thin film (m^2/s); d_{barr}: thickness of the thin film (m) assuming a dry density of MnO_2 crystals of 2×10^6 g/m^3 in the thin film; S: calcite sand surface area (m^2/m^3); n: total porosity in the calcite contactor (adimensional); Ca_{eq}: calcium concentration at equilibrium with calcite at the grain surface.

The model was implemented in the PHREEQC software using a MATLAB interface via IPHREEQC modules (Charlton & Parkhurst, 2011). The equations from Table 3-3 were written in the RATES and KINETICS datablock with 1.0E-06 solving tolerance. The calcite contactor was simulated using the TRANSPORT datablock. Hydraulic properties were defined following the PHREEQC dual porosity feature: mobile porosity of 34%, immobile porosity of 1.2%, dispersivity of 5 cm and exchange factor of 5E-06 s^{-1}. These hydraulic properties were selected based on typical

hydraulic behavior of sand columns (Domenico & Schwartz, 1998). The simulated column had 8 cells. The influent was simulated in the REACTION datablock in which $CaCl_2$, $MnSO_4$ and $NaHCO_3$ were added to reproduce the experimental conditions. Prior to the column simulation, the influent was equilibrated with calcite and with a 300 ppm CO_2 of the atmosphere. The model kinetic constants k_{CAL}, k_{MnCO3} and k_{MnO2} as well as diffusion coefficient D_{barr} were calibrated using the data from the Continuous sorption-dissolution experiment. The calibrated model was used for scenario simulations with different influent manganese concentration and different precipitation hypothesis.

3.2.4 Sorption-dissolution experiments with a blend of calcite and *Corosex™* media

3.2.4.1 Characteristics of synthetic feedwater (SFW) and calcite sand

Synthetic feed water (SFW) was prepared using the same procedure described in section 3.2.1.1. Commercially available *Corosex™* (3.6 g/cm^3) media was purchased from Clack Corporation, Windsor, Wisconsin, USA. To determine the particle size distribution and accordingly the representative diameter of the grains, sieving analysis was executed on *Corosex™* sample. The Fig. 3.5. demonstrates the results of sieving analysis and based on the results, the median diameter (D_{50}) of 1.6 mm was chosen. Furthermore, the effective diameter (D_{50}) of the *Corosex™* grains is 1.4 mm as reported by Clack Corporation, Windsor, Wisconsin, USA. The main characteristics of *Corosex™* media are summarized in Table 3.4.

Table 3-4: Magnesium oxide (*Corosex™*) media characteristics

Filter media	D_{50}(1) (mm)	D_{10}(3) (mm)	Purity (2) (%)	Specific gravity (3) (g/cm^3)	Bulk density (3) (kg/m^3)	Surface area (4) (m^2/g)	Other impurities (3)
Corosex™ (MgO)	1.6	1.4	98	3.6	1 200	0.390	0.4 % Fe 1.1 % Ca

(1) Measured in the laboratory using sieving
(2) Determined by Inductively Coupled Plasma-Optical Emission Spectrometry (ICP-OES, model iCAP 6000, Thermo Instruments Inc) after nitric acid acidification
(3) Provided by the supplier (Clack Corporation, Windsor, Wisconsin, USA)
(4) Data provided via BET measurement (The BET procedure is described in (Gambou-Bosca & Bélanger, 2016))

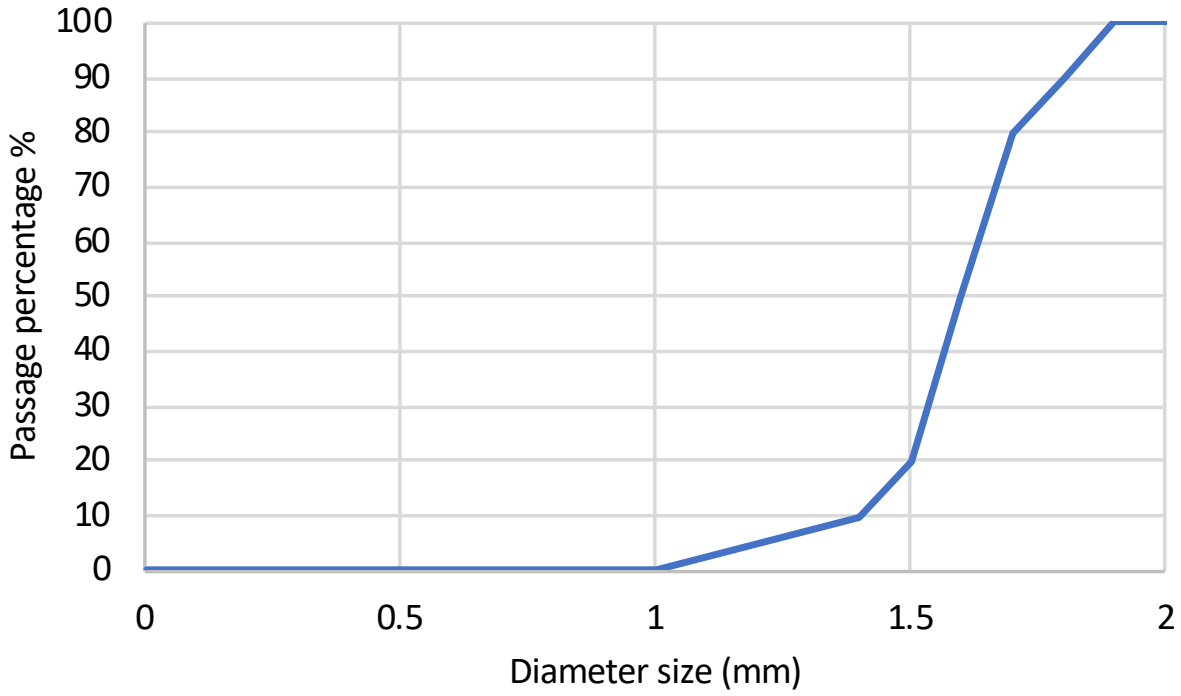

Figure 3-4: The size distribution curve of *Corosex*^{TM} for grain size ranging between 0.8-1.6

3.2.4.2 Experimental set-up and procedure

The same experiment (setup and procedure) as section 3.2.1.2 was carried out. The only difference was that a blend of calcite (i.e., calcium carbonate), mixed with magnesium oxide (MgO) was used instead of only calcite. First, three different ratios of Calcite/ *Corosex*^{TM} (90:10, 80:20, and 70:30) were examined to find an optimum ratio regarding remineralization because the main objective of this section was to solve the problem of the low remineralization which was a limiting factor when only calcite was used. After having chosen the optimum ratio (80:20), the same experiment as section 3.2.1.2 was undertaken to investigate the efficiency of the contactor in remineralization of soft water with simultaneous Mn removal. The Fig. 3.4. shows the filter bed material consists of Calcite and *Corosex*^{TM}.

Figure 3-5: Filter bed material: Calcite (left) and *Corosex*^{TM} (right)

Chapter 4 ARTICLE 1 - IMPACT OF MEDIA COATING ON SIMULTANEOUS MANGANESE REMOVAL AND REMINERALIZATION OF SOFT WATER VIA CALCITE CONTACTOR

This chapter presents the submitted manuscript to the Journal of Water Research on November 7th, 2018.

Impact of media coating on simultaneous manganese removal and remineralization of soft water via calcite contactor.

Hamed Pourahmad[1], Maryam Haddad[1], Dominique Claveau-Mallet[2] and Benoit Barbeau[1,*].

1: Department of Civil, Geological & Mining Engineering, Ecole Polytechnique de Montréal, 2900 boulevard Édouard-Montpetit, Montréal, Québec, Canada H3T 1J4, hamed.pourahmad@polymtl.ca, maryam.haddad@polymtl.ca, benoit.barbeau@polymtl.ca

2: Department of Chemical Engineering, McGill University, 3610 University Street, Montréal, Québec H3A 0C5, Canada, dominique.claveau-mallet@mail.mcgill.ca

* corresponding author: Benoit Barbeau

Abstract

The aim of this study was to investigate the negative impact of newly-formed manganese (Mn)-layer on calcite dissolution in a long-term operation of a calcite contactor. Simultaneous removal of Mn and remineralization of soft water in an up-flow calcite contactor was conducted and led to a progressive loading of Mn into the calcite matrix. The calcite contactor demonstrated high Mn removal efficiency; however, the hardness release decreased from 32 to 20 mg $CaCO_3$ L^{-1} after 600 h of operation in high Mn concentration condition. For an elevated Mn concentration (i.e. 5 mg Mn L^{-1}) in the feed water, the coated layer was mainly composed of Mn which inhibits the mass transfer from the calcite core to the liquid phase. The superficial layer was identified as 5.2% Mn oxides (MnOx) by X-ray photoelectron spectroscopy (XPS). Therefore, it is postulated that Mn removal starts with an ion exchange sorption reaction between soluble Mn^{2+} from aqueous phase and Ca^{2+} from the $CaCO_3$ matrix which is followed by a slow recrystallization of $MnCO_3$ into MnO_2. On the

other hand, when the Mn content in the feed water was lower (i.e. 0.5 mg Mn L^{-1}), a considerably lower amount of MnOx was detected on the coated media. For all the examined conditions, the formation of this coating improved Mn removal due to the autocatalytic nature of adsorption/oxidation of dissolved manganese by MnOx. A mechanistic model based on calcite dissolution and progressive formation of a MnO_2 layer was implemented in PHREEQC software to predict the reduction in hardness release expected in long-term operation. The model was calibrated with experimental data and resulted in realistic breakthrough curves. In order to accurately predict the pH of the effluent stream, a slow-rate recrystallization of $MnCO_3$ into MnO_2 was implemented (compared to fast precipitation of MnO_2 or absence of MnO_2 formation).

Keywords

Calcite Contactor, Manganese Removal, Soft water Remineralization, Groundwater supplies, sorption, PHREEQC

Highlights

- Calcite was able to remove > 95% of Mn^{2+} in a long-term operation, reaching effluent concentration below 45 μg Mn^{2+} L^{-1}.
- In very high Mn concentration (5.0 mg Mn^{2+} L^{-1}), sorbed Mn first incorporates into calcite matrix and then recrystalizes into MnOx.
- Newly-formed MnOx layer deteriorates calcite dissolution.
- In high Mn content (0.5 mg Mn^{2+} L^{-1}), sorbed Mn incorporates into calcite matrix.

4.1 Introduction

Corrosion control is an important water treatment objective, too often neglected by water treatment engineers designing a new water treatment system. Addition of caustic soda, soda ash, lime (with or without carbon dioxide) and various corrosion inhibitors are the main corrosion control techniques used in municipal water treatment sector (Withers, 2005). For domestic purposes and small water systems, filtration through a bed made of mainly calcite (i.e. calcium carbonate is regularly used as a remineralization strategy, which is referred to as calcite or limestone contactor. Remineralization of the finished water from desalination plants is another common application of this process. Calcite dissolution, as described by Eq. 1, provides calcium hardness and bicarbonate alkalinity.

$$CaCO_3 + CO_2 + H_2O \rightarrow Ca^{2+} + 2\ HCO_3^- \qquad \text{(Eq. 1)}$$

Several researches have shown that calcite filtration is a reliable remineralization method as no continuous chemical addition is required and calcite is inexpensive, readily available, safe and easy to store and operate (Shemer et al., 2013; Van Der Laan. H., 2016). Another interesting advantage

of calcite lies in its ability to sorb divalent metallic cations (Me^{2+}) on its surface (Aziz & Smith, 1996; Franklin & Morse, 1983). Due to its superior efficiency, a number of researchers recommended using calcite media for manganese removal from acid mine drainage (Aziz & Smith, 1992, 1996; Thornton, 1995; Zachara et al., 1991). In drinking water applications, manganese removal is also a common treatment objective. The occurrence of Mn in drinking water causes aesthetic and operational issues (Tobiason et al., 2016). Manganese is under review in Canada and the USA for a possible health-based regulation given the increased evidence of manganese neurotoxicity, especially for children (Bouchard et al., 2011; Dion et al., 2018). Thus, efficient removal of Mn from drinking water is crucial.

Mn removal from drinking water sources can be carried out by different methods (Tobiason et al., 2016). A common municipal water treatment technique for Mn removal relies on its oxidation by a strong chemical followed by precipitation and particle removal (Kothari, 1988). As on-line chemical injection is challenging in small-scale applications, point-of-entry (POE) catalytic filtration with intermittent regeneration or POE cationic ion exchange (IX) coupled with point-of-use reverse osmosis are two widely implemented options to remove Mn in domestic applications (Carrière et al., 2011). Nonetheless, the risk of Mn leaching from improperly operated catalytic filters, the high salt consumption for IX regeneration and the considerable amount of brine waste production, which pollutes the environment, are common drawbacks of these methods (Barbeau et al., 2011; Carrière et al., 2011). As an alternative, we recently proposed the use of chlorine resistant and back-washable hollow fiber nanofiltration (HFNF) membranes for the removal of Mn from domestic groundwater supplies (Haddad et al., 2018). We concluded that even though HFNF application can be an appealing solution for the effective removal of Mn and Fe, non-selective rejection properties of the HFNF membranes would result in a corrosive treated water. Therefore, the HFNF process should be coupled with a polishing step, such as a calcite contactor, to adjust the hardness level of its soft permeate. This final post-treatment can also further reduce the dissolved Mn traces which was not completely rejected by the HFNF membranes (Haddad et al., 2018).

Calcite ($CaCO_3$)-Mn interaction and particularly the fate of various phases in the complex system of $CaCO_3$-$MnCO_3$-H_2O has been extensively documented in the literature (Franklin & Morse, 1983; Kothari, 1988; McBride, 1979; Pingitore et al., 1988; Silva et al., 2012; Thornton, 1995; Zachara et al., 1991). In 2010, Silva et al. studied the interaction of Mn^{2+} and calcite and claimed that the nucleation of the discrete phase of rhodochrosite (i.e., $MnCO_3$) takes place at the surface of the calcite media (Silva et al., 2010). By contrast, a number of researchers indicated that a dilute solid solution of Mn^{2+}-$CaCO_3$ is formed at the surface due to the displacement of Mn^{2+} in the calcite matrix (Comans & Middelburg, 1987; McBride, 1979; Pingitore et al., 1988). Furthermore, since no adsorption maximum is determined in the abovementioned studies, it can be deduced that both precipitation-adsorption were involved in the interaction between Mn and calcite (McBride, 1979). The most commonly accepted kinetic rate law for Mn and calcite interaction includes an initial rapid uptake of the trace metal (i.e. Mn^{2+}) followed by a relatively slow formation of a solid solution expressed as $Mn(x)Ca(1-x)CO_3$; where the composition (x) changes between the original solid and precipitate of the sorbate while it is gradually formed (Farley et al., 1985; McBride, 1979; Zachara

et al., 1991). The initial rapid step is generally linked to an adsorption reaction while the following slow uptake is mainly attributed to the formation of solid solution and removal by surface precipitation. A number of researchers claimed that at a low aqueous concentration, metals only incorporate into the surface of calcite by adsorption with no solid solution formation (Comans & Middelburg, 1987; Franklin & Morse, 1983; McBride, 1979; Zachara et al., 1991). In 1991, Zachara and coworkers reported that metals with ionic radii smaller than Ca were more prone to sorb on calcite (Zachara et al., 1991) which favors the theory of calcium displacement. Finally, it should be noted that Mn^{2+}, once integrated into the solid matrix of calcite, exhibits a very slow desorption rate which favors the application of calcite for Mn sorption in the field of water treatment (McBride, 1979; Zachara et al., 1991).

The three most common calcite dissolution models are Plummer, Parkhurst, Wigley (PWP) (1978) Yamauchi (1987) and Letterman (1987) (Letterman et al., 1987; Plummer et al., 1979; Plummer et al., 1978; Yamauchi et al., 1987). In the PWP and Yamauchi models, it is assumed that the flow is turbulent and the process is very fast; thereby, the calcite dissolution is controlled only by surface reactions, i.e., diffusional mass transport is neglected (Ghanbari, 2018; Plummer et al., 1979; Yamauchi et al., 1987). On the other hand, in the Letterman model, mass transfer is the key controlling mechanism used to predict calcite dissolution (Letterman et al., 1987). However, none of these models account for the potential negative impact on calcite dissolution arising from the precipitation of manganese on its surface. Despite the fact that there are several comprehensive studies pertaining to both the implementation of calcite contactors as a reliable and straightforward remineralization and corrosion control technique and Mn adsorption on the surface of calcite, to the best of our knowledge, the significance and fate of sorbed Mn on the overall performance of a calcite contactor in a long-term operation has not received enough attention. In this regard, the primary goal of this research effort is to determine the effect of Mn-coating on calcite dissolution rate and model the long-term behavior of a calcite contactor operated for drinking water remineralization. The outcome of this study enables us to gain a clear insight of the fate and significance of sorbed Mn at calcite surface and helps in the design of a simple and efficient polishing step for the soft permeate from HFNF processes.

4.2 Materials and methods

4.2.1 Calcite media and synthetic feed water

Synthetic feed water (SFW) was prepared by dissolving analytical grade (>99% pure) $MnSO_4$ (Fisher Scientific, NJ, USA) in ultra-pure (i.e., Milli-Q™) water. Commercially available calcite (2.68 g/cm^3) media was purchased from Imerys Marble Inc. (Sahuarita, AZ, USA) and then dry-sieved to calculate the median diameter (D_{50}). The main characteristics of calcite media are summarized in Table 4-1.

Table 4-1: Calcite media characteristics

(1) Measured in the laboratory using sieving

Filter media	**D_{50} (1) (mm)**	**Purity (2) (%)**	**Specific gravity (3) (g/cm^3)**	**Bulk density (3) (kg/m^3)**	**Porosity (3) (ε)**	**Surface area (4) (m^2/g)**	**Other impurities (3)**
Calcite ($CaCO_3$)	0.4	99.70	2.68	1500	0.42	0.371	0.3 % Mg

(2) Determined by Inductively Coupled Plasma-Optical Emission Spectrometry (ICP-OES, model iCAP 6000, Thermo Instruments Inc) after nitric acid acidification
(3) Provided by the supplier (Imerys Marble Inc, Sahuarita, AZ, USA)
(4) Data provided via BET measurement (the BET procedure is described in (Gambou-Bosca & Bélanger, 2016))

4.2.2 Experimental design

Two consecutive experimental phases and a single modeling phase were adopted. In the first phase, we determined the overall performance of a calcite contactor for the removal of Mn and remineralization of SFW using two initial concentrations of Mn (i.e. 0.5 and 5 mg Mn L^{-1}). Based on the results obtained from this phase, the objective of the second phase was to investigate the effect of Mn loading on calcite dissolution rate using continuous desorption-dissolution experiments in smaller columns. To this end, we transferred the media from the loaded column used for first phase to 4 mini-columns and operated them for five days in a continuous mode while feeding them with ultra-pure water. As for the final phase, the long-term efficiency of a calcite contactor was modeled based on calcite dissolution, Mn precipitation and filter clogging. The model was implemented in PHREEQC.

4.2.3 Continuous sorption-dissolution experiments

In Phase 1, sorption-dissolution experiments were conducted on calcite media in order to assess the efficiency of a calcite contactor for both remineralization and partial Mn removal. The assays were carried out at room temperature (i.e. 23 ± 2 °C) in two parallel cylindrical acrylic columns (1.3 m height and 31.75 mm internal diameter) filled to a height of 80 cm with fresh calcite media and continuously fed with SFW containing 0.5 mg Mn L^{-1} (column A) or 5 mg Mn L^{-1} (column B), respectively. The flow rate was set at 31.5 ml/min which translates into empty bed contact time (EBCT)=10 m in the second valve (at height of 40 cm) and 20 m in the effluent. It should be noted that these concentrations represent either high or very high Mn conditions in groundwater supplies (Health-Canada, 2016). A schematic illustration of the sorption-dissolution set-up is shown in Fig. 4-1. Throughout the sorption-dissolution assays, samples were collected from four sampling points located at different heights and therefore representing increasing EBCTs. Samples were analyzed

to determine Mn^{2+} concentration, pH and hardness, immediately after their collection. Hardness was measured by titration (Standard methods, Hardness (2340)/EDTA Titrimetric Method) while acidified manganese samples were analyzed by ICP-AES (Thermo-Fisher, ICAP 6000). Details of the ICP sample preparation and the applied measurement procedure can be found elsewhere (Haddad et al., 2018).

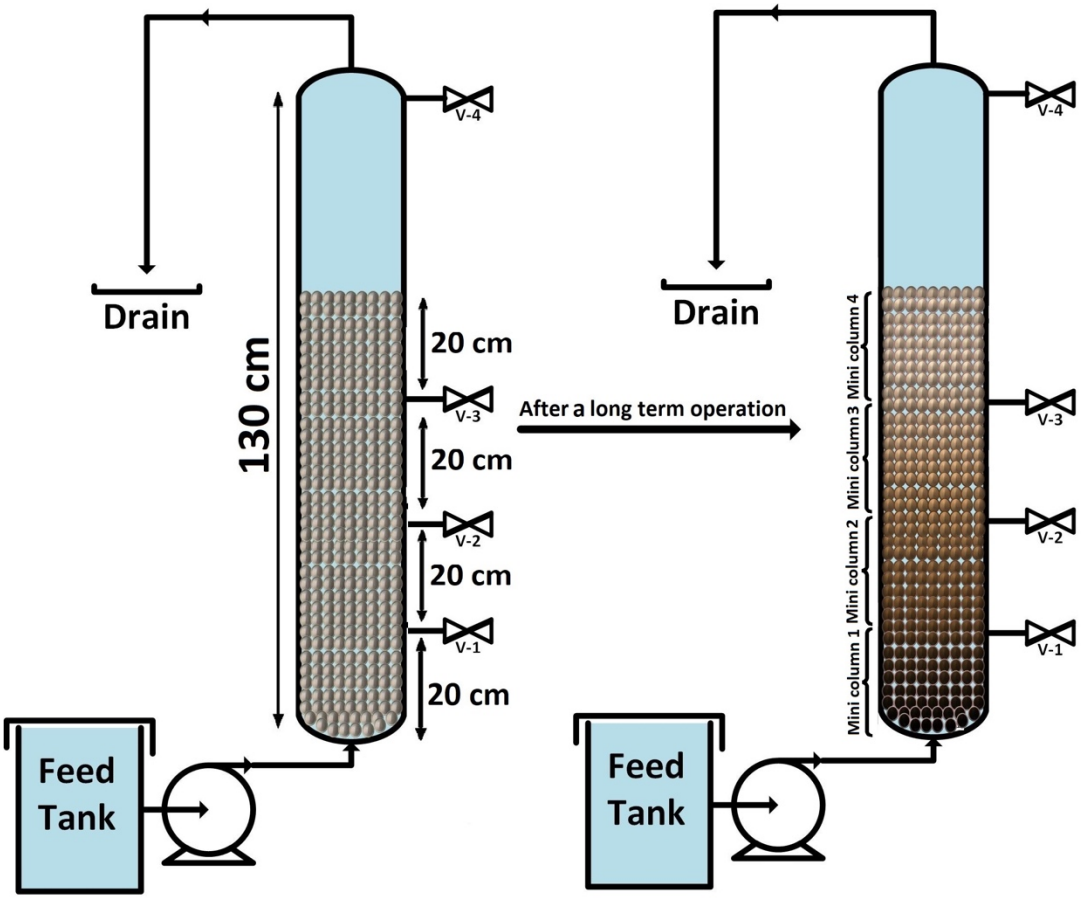

Figure 4-1: Schematic illustration of the continuous sorption-dissolution set-up

4.2.4 Characterisation of calcite Mn-loaded media

After a long-term operation (approximately 800 h) of sorption-dissolution columns, samples of the Mn-loaded calcite media were collected from different depths of the column B for further analysis. Scanning Electron Microscope (SEM), Energy Dispersive X-ray Analysis (EDX) and X-ray Photoelectron Spectroscopy (XPS) were applied to characterize the media before and after loading and to determine the nature of the deposits found over the surface (Detailed description of each of these analyses are provided in the appendix). To determine the quantity of Mn loading on calcite, pre-weighted samples (160 mg of) of the dried loaded media (with different Mn content) were digested in 15 mL of 10% (wt.) HNO_3. Following a complete dissolution, Mn concentrations were measured by means of an ICP-AES.

4.2.5 Desorption experiment and impact of Mn coating on calcite dissolution

In order to investigate the Mn desorption rate, column B (Fig. 4-1) was fed with Milli-Q water for 120 h and samples were collected from two sampling points located at different heights and therefore representing increasing EBCTs (i.e. 10 and 20 m). Then, the impact of Mn loading on calcite dissolution and Mn sorption was tested by transferring the Mn-loaded media from sorption-dissolution experiments to four mini-columns (20 cm media height and 1.5 cm internal diameter) with increasing Mn loadings ranging from 0 to 15 mg Mn g^{-1} of media (Table 4-2). The first column contained fresh calcite media and was considered as the control case. The columns were fed with Milli-Q water for 72 h. Samples were frequently taken from the influent/effluents and characterized for Mn^{2+} content, hardness level and pH according to the methods described above.

Table 4-2: Mn loading in the different mini-columns

# Columns	Column 1*	Column 2	Column 3	Column 4	Column 5
Mn content of the media (mg Mn/g media)	0	1.06	2.13	4.02	14.97

* The control column with fresh calcite media

4.2.6 Batch sorption experiments on Mn-loaded media

Experiments were carried out at T = 23 °C to study the effect of Mn loading on calcite dissolution and investigate the ability of the highly Mn-loaded calcite (collected from the bottom of the large column (i.e. column B in Fig 4-1)) in further removal of Mn^{2+}. The sorption studies were performed by adding 10 g L^{-1} of Mn-loaded media to 200 mL flasks with various Mn^{+2} concentrations (0.0, 0.1, 1.0 and 10 mg Mn L^{-1}). Throughout the sorption assays, the flasks were shaken (using Max Q2508 Thermo-Fisher shaker) at 150 rpm. At predetermined contact times (i.e. 15 m, 1 h, 12h, 24 h, 48 h and 7d), a flask from each Mn concentration was removed, settled for 1-min and the supernatant was filtered using a 0.45 μm membrane filter (Supor ®PES Membrane Disc Filters, Pall, US) prior to Mn, hardness and pH measurements.

4.2.7 Model description and numerical simulations

The applied model in this study consisted of the equations for calcite dissolution, $MnCO_3$ formation (by ionic exchange between Ca^{2+} and Mn^{2+}) as well as the slow recrystallization of $MnCO_3$ into MnO_2 as indicated in Table 4-3. In this regard, a simple calcite dissolution rate based on calcite saturation index was defined. In (Claveau-Mallet et al., 2017), the successful application of the selected rate is reported for phosphorus precipitation in granular reactors. The calcite equilibrium constant was set at $pK_{spCAL} = 8.48$ according to standard geochemical database for crystalline calcite (Parkhurst & Appelo, 1999). The formation of MnO_2 was assumed according to mineralogical observations performed in this study (presented in the result section). The $MnCO_3$ precipitation rate was set as a first order reaction without $MnCO_3$ saturation assuming that

autocatalytic sorption took place onto previously formed seeds. The $MnCO_3$ precipitation kinetic constant was increasing gradually to account for the increase of seeds. A saturation term of 1.8×10^{-7} M (10 μg Mn L^{-1}) was included in the rate to represent the lowest residual concentration observed in the effluent of the calcite contactor.

Calcite dissolution was presumed to be progressively limited by the formation of a thin MnO_2 film over the calcite grains. The diffusion of Ca^{2+} and CO_3^{2-} ions through the film was modelled based on Fick's law. At each iteration step, both dissolution and diffusion rates were calculated, and only the smallest rate was applied (which resulted in dissolution control at first and diffusion control afterward).

Table 4-3: Applied equations for calcite dissolution and manganese removal modeling

Processes	Stoichiometry					Rate law
	Ca^{2+}	CO_3^{2-}	Mn^{2+}	H^+	e^-	
Calcite dissolution	-1	-1				$r_{CAL} = k_{CAL} log\left(\frac{\{Ca^{2+}\}\{CO_3^{2-}\}}{K_{spCAL}}\right)$
Calcite diffusion through MnO_2 thin film	-1	-1				$r_{diff} = \frac{0.001 D_{barr}\left(K_{spCAL} - \{Ca^{2+}\}\{CO_3^{2-}\}\right)}{d_{barr}}\left(\frac{S0.001(1-n)}{n}\right)$
$MnCO_3$ formation by ionic exchange from calcite matrix	+1		-1			$r_{MnCO3} = k_{MnCO3}([Mn^{2+}] - 1.8 \times 10^{-7})$ $k_{MnCO3} = 10^{(A * X_{Mn} - B)}$ Note: 1.8×10^{-7} is a saturation term describing the min concentration of Mn^{+2} (based on experimental measurements)
Recrystallization of $MnCO_3$ into MnO_2		+1		+4	+2	$r_{MnO2} = k_{MnO2}([MnCO_3] - [MnO_2])$

X_{Mn}: total Mn precipitated in the calcite contactor (mol L^{-1} void volume); A and B: constants for seeding; D_{barr}: diffusion coefficient in the thin film (m^2/s); d_{barr}: thickness of the thin film (m) assuming a dry density of MnO_2 crystals of 2×10^6 g/m^3 in the thin film; S: calcite sand surface area (m^2/m^3); n: total porosity in the calcite contactor (adimensional); Ca_{eq}: calcium concentration at equilibrium with calcite at the grain surface.

The model was implemented in the PHREEQC software using a MATLAB interface via IPHREEQC modules (Charlton & Parkhurst, 2011). The equations from Table 4-3 were written in the RATES and KINETICS datablock with 1.0E-06 solving tolerance. The calcite contactor was simulated using the TRANSPORT datablock. Hydraulic properties were defined following the PHREEQC dual porosity feature: mobile porosity of 34%, immobile porosity of 1.2%, dispersivity of 5 cm and exchange factor of 5E-06 s^{-1}. These hydraulic properties were selected based on typical hydraulic behavior of sand columns (Domenico & Schwartz, 1998). The simulated column had 8

cells. The influent was simulated in the REACTION datablock in which $CaCl_2$, $MnSO_4$ and $NaHCO_3$ were added to reproduce the experimental conditions. Prior to the column simulation, the influent was equilibrated with calcite and with a 300 ppm CO_2 atmosphere. The model kinetic constants $k_{CAL,}$ k_{MnCO3} and k_{MnO2} as well as diffusion coefficient D_{barr} were calibrated using the data from the Continuous sorption-dissolution experiment. The calibrated model was used for scenario simulations with different influent manganese concentration and different precipitation hypothesis.

4.3 Results and discussion

4.3.1 Media characterization

The fresh calcite and loaded calcite produced in the long-term operation of the contactor fed with 5 mg Mn L^{-1} were characterized by SEM, EDX and XPS. Table 4-4 depicts the SEM images of the calcite surface before and after Mn sorption at 1000X as well as EDX results obtained at 250X magnification. SEM images show the structure of the coating at calcite surface. By comparing the SEM images of the fresh and Mn loaded media, one can note that the loaded media exhibited a smoother surface. The EDX results demonstrated no Mn peak in fresh media (0%); whereas a gradual increase in the Mn content (≤ 15%) of the loaded media was observed. Thus, it can be presumed that the Mn was progressively coated on the calcite surface, forming a layer of Mn which can inhibit the mass transfer from the calcite core to the liquid phase.

The nature of the newly formed residue was investigated by XPS analysis. Even though the Mn2p3 peak for $MnCO_3$ is expected at a binding energy (BE) around 640.4 eV (Table 4-5) (Baer et al., 1991), the Mn2p3 peak was observed at a BE of 641.7 eV which corresponds to the Mn^{3+} and Mn^{4+} oxides and hydroxides. It should be noted that a number of researchers reported the incorporation of Mn into calcite matrix and formation of $MnCO_3$ (Pingitore et al., 1988; Silva et al., 2012; Silva et al., 2010; Silva et al., 2012); however, based on the XPS results, the newly formed residue was not solely $MnCO_3$ as the presence of Mn oxides and hydroxides were detected at calcite surface. The detection of MnOx formation on the surface was supported by the pH measurements in the effluent which were lower than what would have been expected in the case of sole formation of $MnCO_3$. The formation of MnOx is expected to slightly acidify the effluent. Therefore, it was postulated that Mn sorption starts with an ion exchange reaction between soluble Mn^{2+} from aqueous phase and Ca^{2+} from the $CaCO_3$ matrix which is followed by slow recrystallization of $MnCO_3$ into MnO_2.

Table 4-4: SEM images and EDX analyses of calcite media drawn from different Mn loadings on the calcite media.

Media specifications	SEM image (1000X)	EDX Spectrum (250X)

Mini-column #1 (Control case) (0 mg Mn g^{-1} calcite)	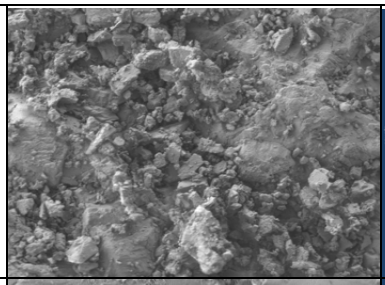	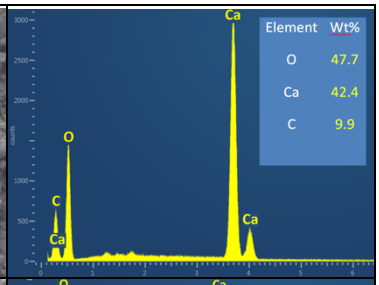
Mini-column #2 (1.06 mg Mn g^{-1} calcite)	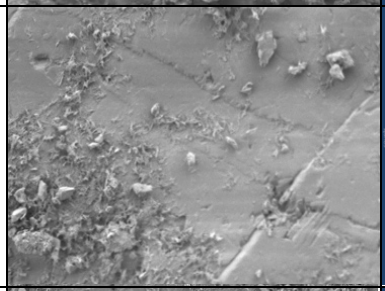	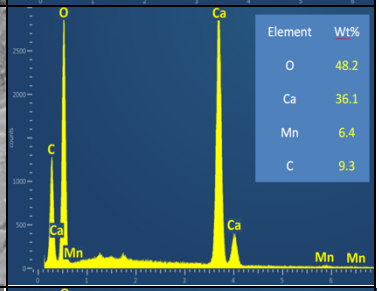
Mini-column #3 (2.13 mg Mn g^{-1} calcite)	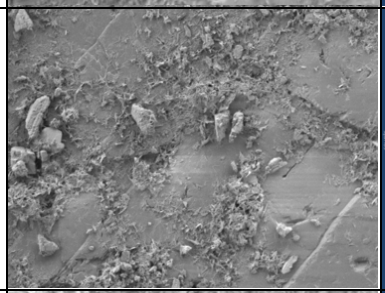	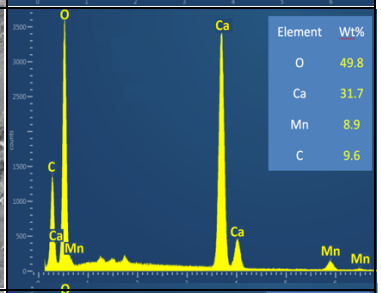
Mini-column #4 (4.02 mg Mn g^{-1} calcite)	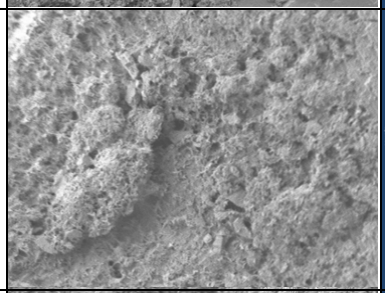	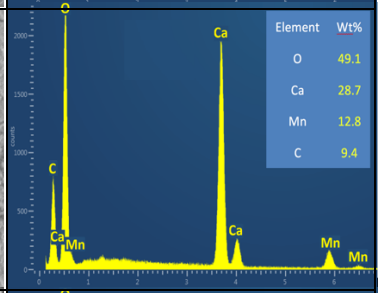
Mini-column #5 (14.97 mg Mn g^{-1} calcite)	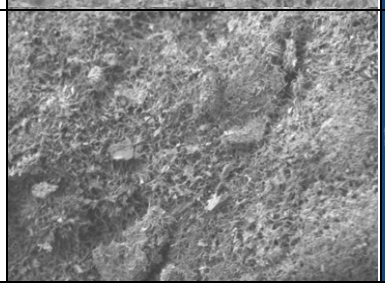	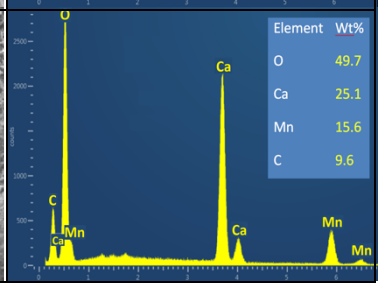

Table 4-5: High resolution XPS spectra for Mn loaded calcite

Name	BE (eV)	Identification	Relative atomic %	
			Fresh calcite	Mn-loaded calcite
C1s	285.0	C-C	15.7	11.5
	288.7	O-C=O	1.2	2.4
	290.1	R-CO_3	12.9	10.7
Ca2p3	347.3	$CaCO_3$	12.7	12.0
O1s	529.9	MnO_2 or other Mn oxide. Other metal oxide.		9.8
	530.5	Metal oxides	4.6	
	531.9	R-CO_3, metal-OH, Si-O	52.9	48.4
Mn2p3	641.7	MnO_2, Mn_2O_3, or MnO(OH)	---	5.2

4.3.2 Effect of initial Mn concentration on long-term operation of a calcite contactor

Fig 4-2a shows Mn^{2+} concentration profiles inside the calcite contactors fed with SFW containing 0.5 or 5 mg Mn^{2+} L^{-1} after 800 h of operation. For both tested conditions, the contactors were able to remove over 95% of dissolved Mn from the SFW, reaching effluent concentration below 45 μg Mn^{2+} L^{-1}. This removal efficiency was achieved in the column fed with 0.5 mg $Mn^{2+}L^{-1}$ from the beginning of the operation; nevertheless, the trend was different for the higher initial Mn concentration (i.e. 5.0 mg $Mn^{2+}L^{-1}$): the stable condition was reached after 100 h of operation. Even though Mn breakthrough was not observed in the effluent for any of the two columns after 800 h, hardness release declined after around 600 h of operation when the initial Mn concentration in the feed was 5.0 mg $Mn^{2+}L^{-1}$ (Fig 4-2b).

It is of interest to point out that no significant change of the color of the bed treating 0.5 mg $Mn^{2+}L^{-1}$ was observed, visually. In contrary, the feed with 5 mg $Mn^{2+}L^{-1}$ resulted in a significant change of the bed color (from milky white towards black-brownish) (Fig 4-1). A possible explanation for the observed hardness decline is most likely the effect of MnOx present on the calcite surface, a statement supported by the EDX analysis. After a long-term operation of the contactor, Mn accumulated at calcite surface caused a deterioration of the calcite dissolution due to the coverage of the mass transfer boundary layer with Mn deposits which impeded calcium diffusion from the calcite core through this newly formed layer. Consequently, after the long-term operation calcite cannot be dissolved efficiently and should be replaced by fresh media.

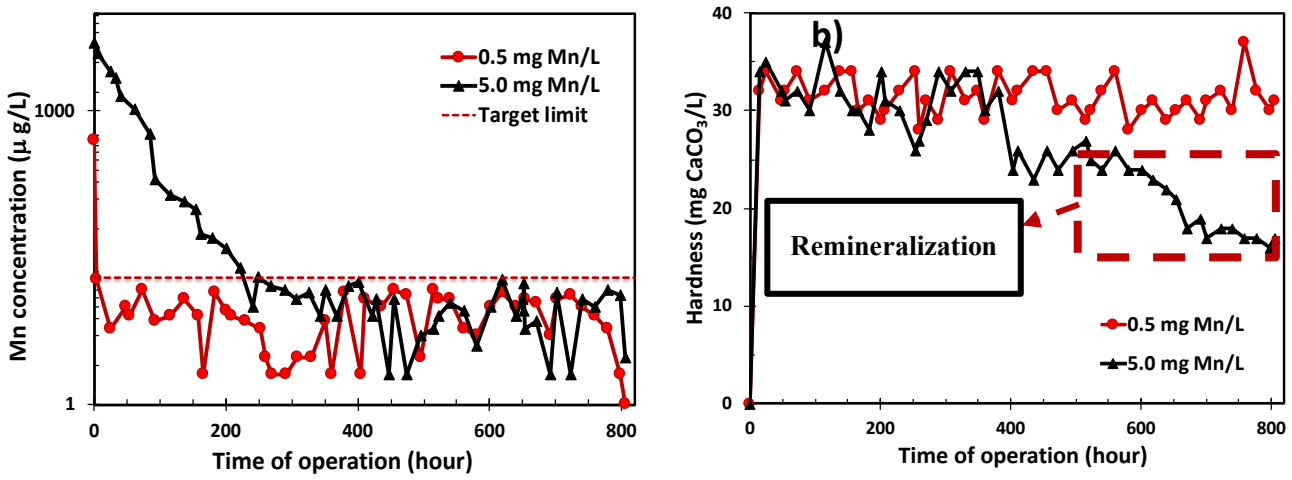

Figure 4-2: Concentrations of a) Mn^{2+} and b) hardness measured over 800 h at the effluents (EBCT=10 min) of calcite contactors fed either with SFW containing 0.5 or 5 mg Mn^{2+} L^{-1}

4.3.3 Effect of Mn loading on calcite dissolution

Fig. 4-3 illustrates the concentration of hardness released from the 5 columns which contained increasing Mn loadings (0 to 15 mg Mn g^{-1} calcite). Indeed, in the case of fresh calcite (0 mg Mn g^{-1} calcite), the hardness release is higher than the Mn loaded calcite (1-15 mg Mn g^{-1} calcite). This phenomenon can be linked to the coating effect of Mn on the calcite surface (Fig. 4-3) which inhibited the dissolution of calcite. Thereby, it can be assumed that a Mn layer was formed in the solid-liquid interface where the dissolution reaction took place and, accordingly, deteriorated the calcite dissolution. As mentioned earlier, the higher the Mn content in the calcite matrix, the lower the calcite dissolution and, subsequently, the lower the hardness release.

In should be pointed out that the highly loaded mini column was fed with Milli-Q water for 120 and 800 h to investigate the Mn desorption rate and determine the impact of the loaded media on the head loss, respectively. Results demonstrated no significant back dissolution of Mn to the aqueous phase; the Mn deposit formed appeared to be very stable. Furthermore, no significant head loss was observed after the long-term operation of the Mn loaded column (i.e. 800 h).

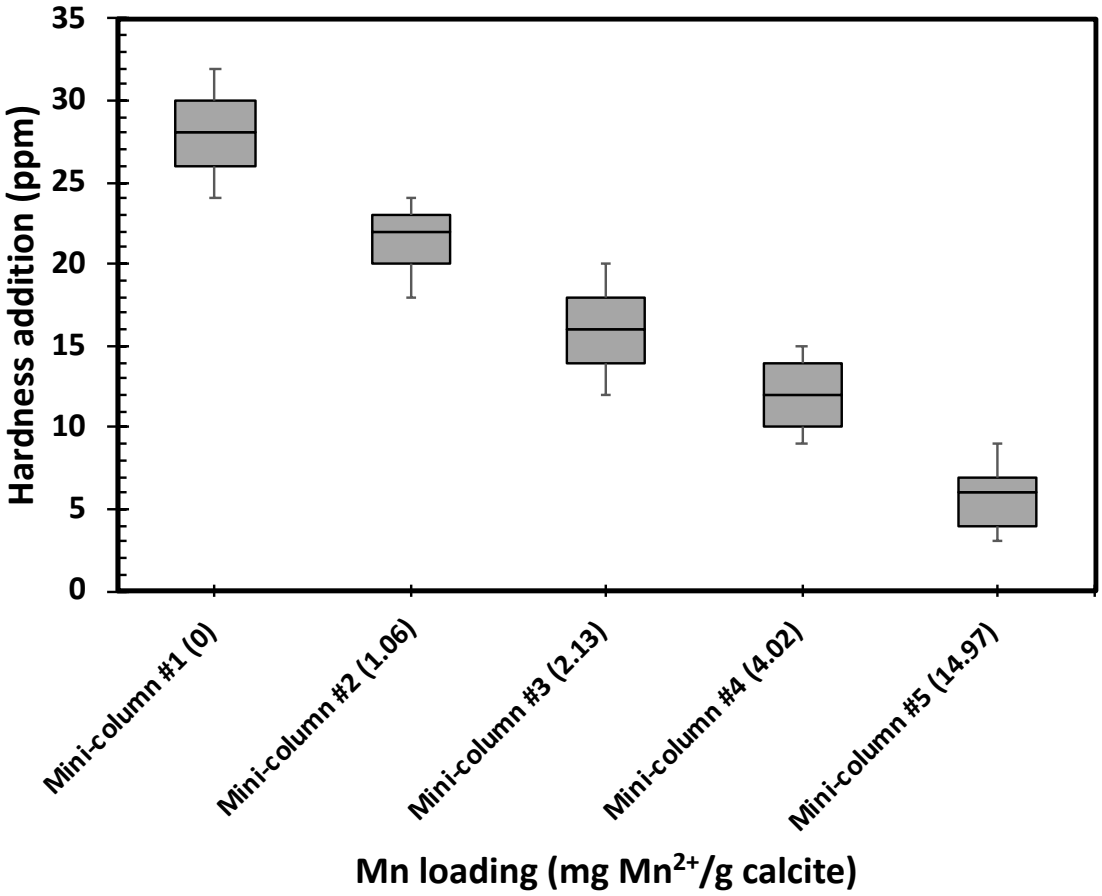

Figure 4-3: Hardness increase achieved by mini-columns containing increased Mn loading on the calcite media (the numbers in parenthesis represent the amount of the Mn loading of media (mg Mn g^{-1}calcite). EBCT = 10 min and the feedwater had no hardness, pH = 6.0 and T = 23 °C.

4.3.4 Mn removal kinetics

Fig. 4-4 presents Mn removal kinetic in a batch reactor containing 10 g L^{-1} of a) fresh calcite and b) highly Mn loaded calcite (i.e. 15 mg Mn g^{-1}calcite). The red constant lines were drawn to demonstrate the point where the equilibrium was reached. As can be seen in Fig. 4-2, for all the examined conditions, the required time to reach a stable Mn sorption regime on calcite surface was similar, regardless of the Mn loading. However, when the Mn-loaded calcite was used, more efficient Mn uptake was observed compared to the fresh calcite. In the case of the fresh media, when the Mn concentration of the feed was increased from 100 to 10 000 µg Mn^{2+} L^{-1}, the Mn removal degree increased from 76% to 91%, respectively. One can note that, the highest Mn removal (≥ 98%) was reached when the calcite was preloaded with 15 mg Mn g^{-1} regardless of the initial Mn concentrations. This observation can confirm that the Mn-formed layer favored the removal of the influent Mn concentration.

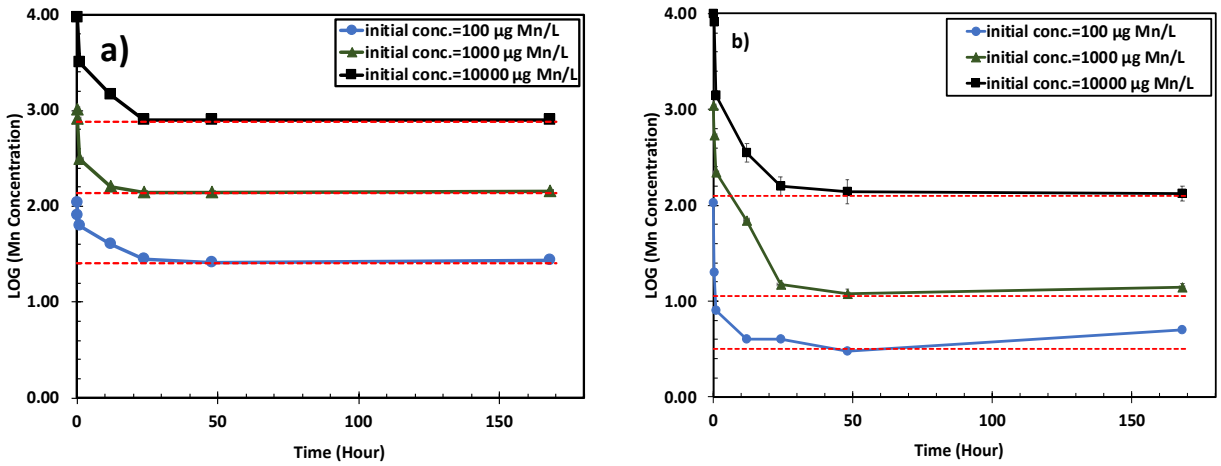

Figure 4-4: Impact of Mn preloading on Mn^{+2} removal by calcite in a mixed batch reactor for a) fresh calcite, b) Mn preloaded calcite (i.e.15 mg Mn g^{-1} calcite)

4.3.5 Prediction of long-term operation of calcite contactor by simulations

The performance of the calibrated model is demonstrated in Figure 4-5 for the column fed with 5 mg Mn L^{-1}. Calibrated parameters were $k_{CAL} = 6 \times 10^{-6}\ M.s^{-1}$, $k_{MnCO3} = 10^{9.35X_{MnO2}-2.95}\ M.s^{-1}$, $k_{MnO2} = 5 \times 10^{-8}\ M.s^{-1}$ and $D_{barr} = 2 \times 10^{-11}\ m^2.s^{-1}$. The simulated Mn molar repartition near the outlet of the column was 10% as MnO_2 and 90% as $MnCO_3$ in the $CaCO_3$ matrix. The calibrated model resulted in good reproduction of Mn experimental data. The model captured the hardness decrease, though the simulated decrease slope was slightly smoother than the experimental one. The slight pH drop was captured as well; however, the simulated pH was higher than the experimental pH by 0.3 to 0.7 pH units. The pH discrepancy can be partly explained by the absence of atmospheric CO_2 input at the effluent in the model. The pH of the effluent samples might have been reduced by CO_2 input during processing, as they had a low buffer capacity.

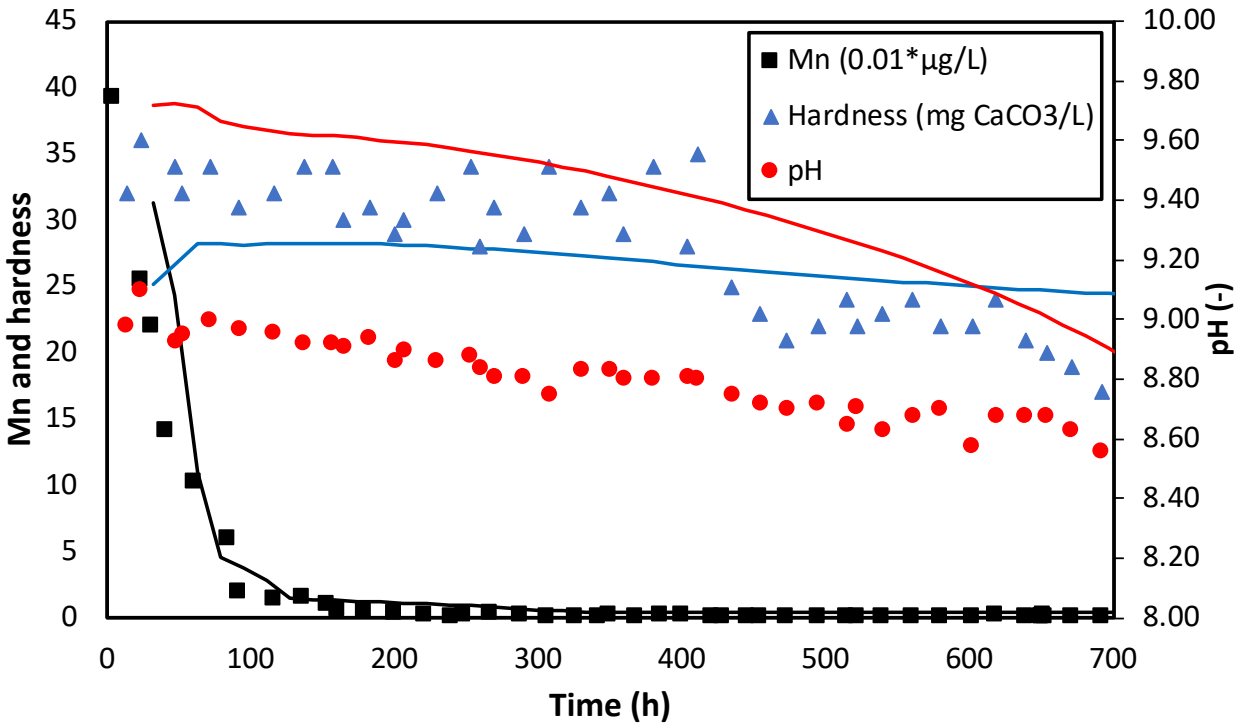

Figure 4-5: Calibrated model predictions for the hardness and manganese data for an EBCT=10 m of the calcite contactor over 700 h of operation. Feed = 5.0 mg Mn L^{-1}. The experimental data are shown by symbols while model predictions are provided as solid lines.

In order to assess the importance of recrystallization reactions in modelling Mn removal by calcite contactors, a sensitivity analysis was performed on the MnO_2 recrystallization rate using an influent with 5000 or 500 µg Mn^{2+} L^{-1} (Fig. 4-6). The recrystallization rate ranged from 5e-9 to 1e-6 M/s, representing a very slow recrystallization kinetic (1% of Mn as MnO_2 on the media close to the outlet) or a very fast recrystallization kinetics (80% of Mn as MnO_2 on the media close to the outlet), respectively.

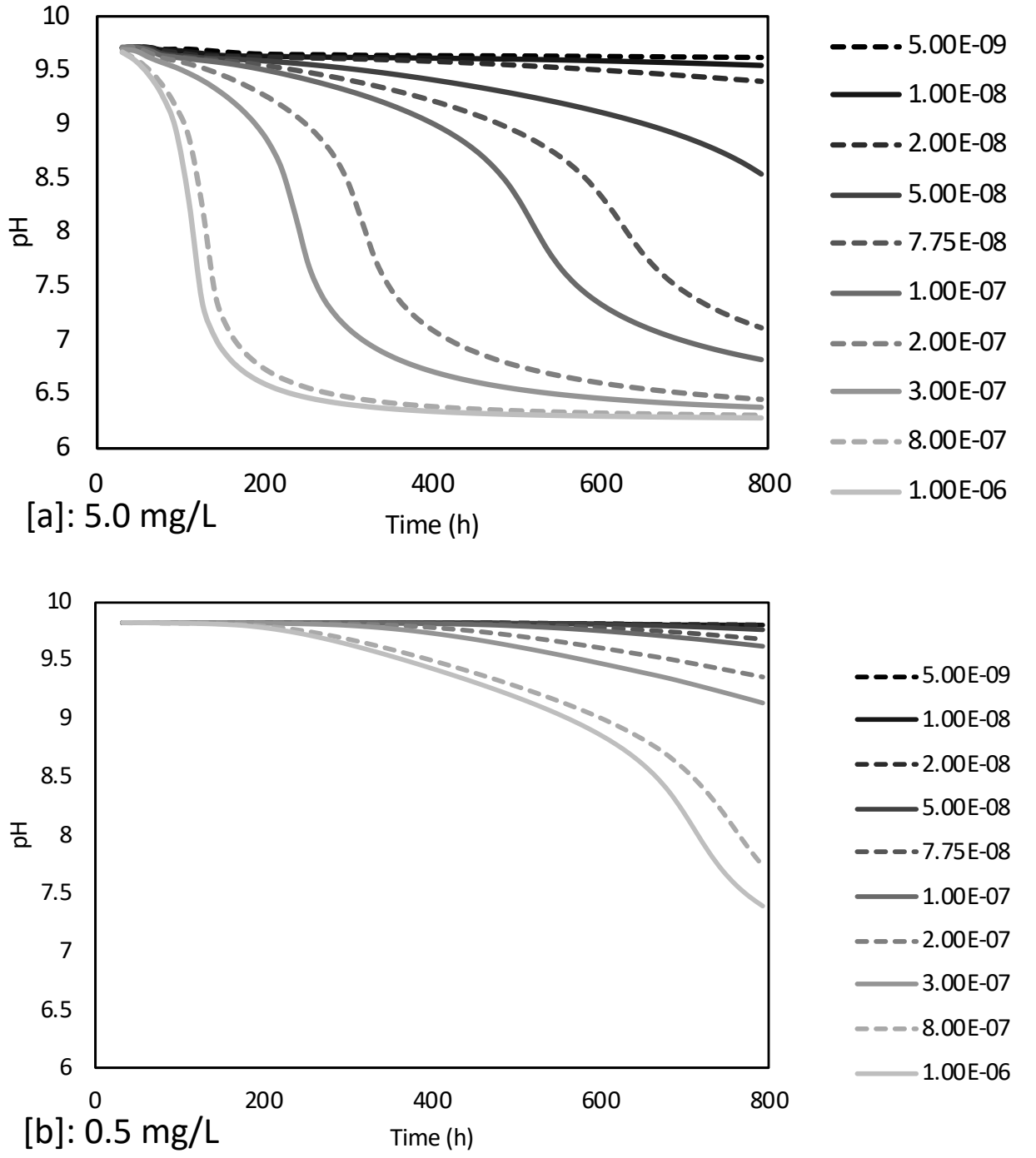

Figure 4-6: Effect of MnO_2 recrystallization rate (M/s, indicated in legend) on pH of the effluent, assuming an influent with a Mn concentration of (a) 5.0 mg Mn^{2+} L^{-1} or (b) 0.5 mg Mn^{2+} L^{-1}.

The pH at the effluent of the calcite contactor was predicted to be highly influenced by the recrystallization rate for both of the Mn initial concentration in the feed water (i.e. 500 and 5000 µg Mn^{2+} L^{-1}). The fastest recrystallization rates resulted in an unrealistically low pH (<6.5 at 5000

µg Mn^{2+} L^{-1}). This indicates that assuming the direct precipitation of MnO_2 or fast recrystallization into MnO_2 were not suitable hypotheses for modelling the calcite contactor. In the course of this study, the proposed modelling strategy consisted of two main steps: (1) fast Mn removal by sorption and (2) slow crystallization of $MnCO_3$ as MnO_2. As shown in Figure 4-5, this strategy employed with proper calibration led to realistic breakthrough curves and $rMnO_2$ content in the contactor. Indeed, the simulated MnO_2 proportion in Mn precipitate for the column fed with 5 mg Mn L^{-1} was over 10%, which was sufficient to be detected by XPS analysis.

In order to apply the proposed model as an efficient tool to design a calcite contactor and predict its exhaustion further investigations are required in terms of calibration (using various initial Mn content in the feed water). In addition, performing additional mineralogical analyses at different points in the contactor and at different times of operation are recommended to substantiate the recrystallization hypothesis. Although implementation of solely calcite media resulted in effective Mn removal, in absence of CO_2 injection to the calcite column, the targeted hardness level (30 mg $CaCO^3$ L^{-1}) was not achieved when Mn was very high in the feed. Thereby, in the future work, the dissolution behavior of a blend of calcite/ *Corosex*^{TM} will be studied by running a long-term calcite/ *Corosex*^{TM} contactor.

4.4 Conclusion

This study set out to determine the adverse impact of newly-formed manganese (Mn)-layer on calcite dissolution in a long-term operation of a calcite contactor. The main findings can be summarized as follow:

- Calcite contactor was able to remove over 95% of dissolved Mn in long-term operation (800 h), regardless of the Mn initial concentrations.
- The targeted hardness level of the effluent water (> 30 mg $CaCO_3$ L^{-1}) was reached at feed Mn concentration of 0.5 mg L^{-1}. However, with a 5 mg L^{-1} Mn feed, the hardness release target was reached only during 400 h.
- Sorption experiments, XPS and EDX analyses showed that hardness decline was most likely due to the MnOx present on the calcite surface. This phenomenon was linked to the coating effect of Mn on the calcite surface which inhibits the dissolution of calcite. We suggested that an Mn layer was formed in the solid-liquid interface where the dissolution reaction took place and, accordingly, deteriorated the calcite dissolution.
- The implemented modelling strategy consisted of two steps: (i) fast Mn removal by sorption and (ii) slow crystallization of $MnCO_3$ as MnO_2. Including this last step was essential to properly model the observed pH behaviour of the effluent.

Clearly, further investigations will be needed to validate the recrystallization hypothesis via mineralogical analyses at different points in the contactor. In addition, an assessment of a long-

term calcite/ *Corosex*^{TM} contactor to achieve > 30 mg $CaCO_3$ L^{-1} when Mn is very high in the feed water is of interest. Work on those issues is ongoing and will be presented in future papers.

Acknowledgements

This research was supported by the Canadian NSERC Discovery Grant Program (312139). The authors thank Mrs. M. Blais for the ICP-OES measurements carried out at the CREDEAU laboratories (a *Canadian Foundation for Innovation* funded infrastructure), Polytechnique Montreal, Canada.

Chapter 5 **SUPPLEMENTARY RESULTS**

This chapter presents additional results that were not included in the published article in the Chapter 4.

5.1 Impact of EBCT on Mn removal and hardness release

The recommended EBCT for a calcite contactor for remineralization purposes, as mentioned earlier, ranges from 10 to 30 minutes (Bang, 2012; Ghanbari, 2018; Nikolay, 2012). This assertion was validated in the course of this study because apart from remineralization, Mn removal has also to be taken into account. The flow rate was kept constant at 4.8 m/h (63 mL/min) and samples were collected from four sampling points located at different heights (See Fig. 3.2) and therefore, representing increasing empty bed contact times ranging from 10 to 40 minutes. Figure 5.1. shows the effect of EBCT on Mn removal for two columns fed with SFW containing 0.5 mg Mn L^{-1} (column A) or 5 mg Mn L^{-1} (column B), respectively. Experimental results were subjected to repeated measures Analysis of Variance (ANOVA) and paired t-test with the common level of significance set at $p = 0.05$. For the tested EBCTs ranging from 10 to 40 minutes, statistically there is a significant difference ($p = 0.001$ for column A and $p = 0.025$ for column B) in Mn removal efficiency at different EBCTs; however, taking into account the error of measurement (device and manipulation) and the fact that in all the tested conditions, the effluent Mn concentration is below 20 µg Mn /L, an EBCT=10 minutes would be a sufficient EBCT for Mn removal and these differences are not practically meaningful. On the other hand, Fig. 5.2. represents the EBCT effect on remineralization for the two columns (A and B). From an engineering viewpoint, the lowest EBCT in which calcite dissolution equilibrium is reached is favorable. Given that calcite dissolution equilibrium is reached after 10 minutes, an EBCT=10 minutes can be chosen as the optimum contact time required to have both remineralization and Mn removal to an acceptable extent (below 20 µg Mn^{2+}/L and over 30 ppm as $CaCO_3$ hardness addition to SFW).

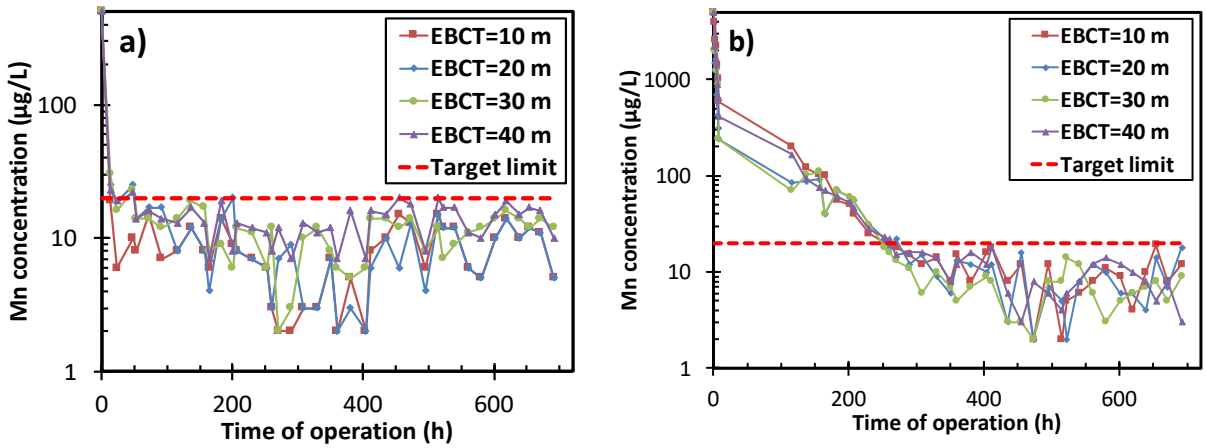

Figure 5-1: EBCT effect on Mn^{2+} removal in a calcite contactor with SFW containing a) 0.5 mg Mn L^{-1} (column A) and b) 5 mg Mn L^{-1} (column B)

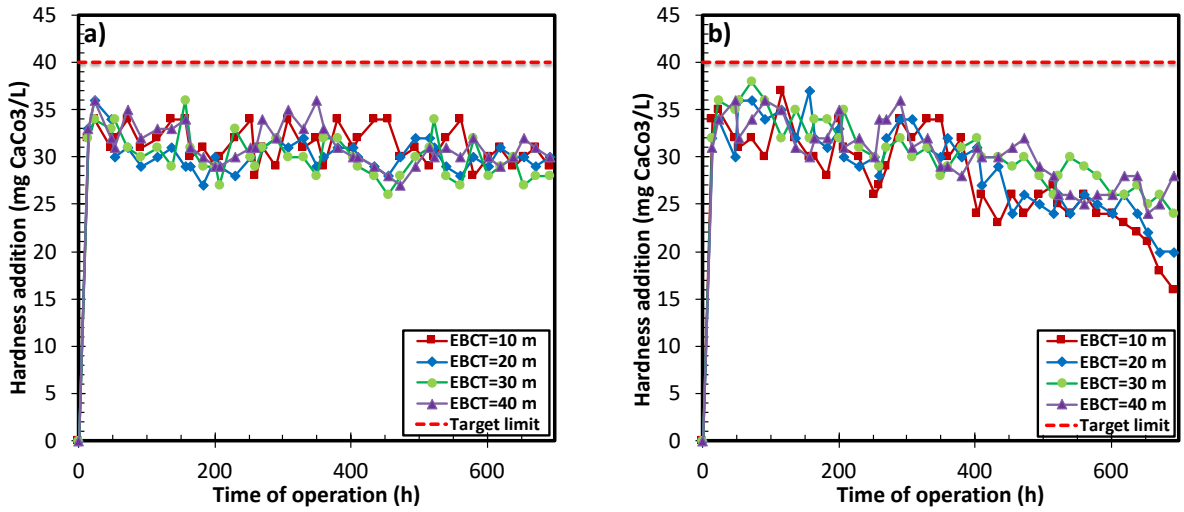

Figure 5-2: EBCT effect on hardness adjustment profile of a calcite contactor with SFW containing a) 0.5 mg Mn L^{-1} (column A) and b) 5 mg Mn L^{-1} (column B)

5.2 Impact of temperature on Mn removal and hardness release

After having chosen the optimum EBCT of 10 min, the effect of temperature on both objectives was investigated in Figure 5.3 (Mn removal) and 5.4 (calcite dissolution). Due to the fact that most adsorption processes are exothermic in nature, temperature is inversely related to the removal of Mn from aqueous solutions via sorption processes (Omri & Benzina, 2012). However, based on the results obtained from laboratory experiments, temperature does not have a pronounced impact on Mn removal on calcite surface and calcite dissolution to the liquid bulk. Furthermore, repeated measures Analysis of Variance (ANOVA) with the common level of significance set at $p = 0.05$ were performed on experimental data. The results confirmed the above-mentioned statement ($p = 0.2$ for column #A and $p = 0.32$ for column #B for Mn removal and $p = 0.52$ for column #A and $p = 0.47$ for column #B for calcite dissolution).

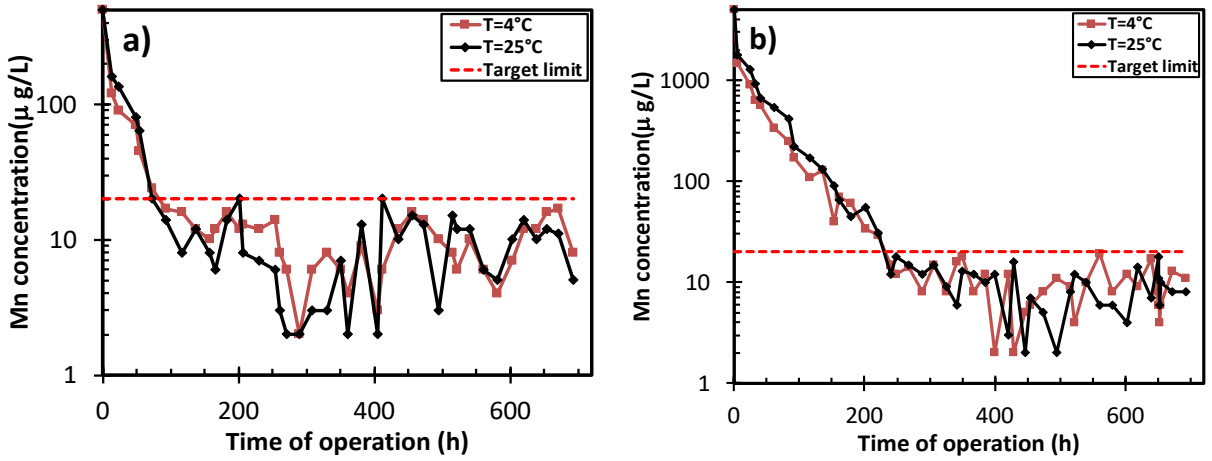

Figure 5-3: Temperature effect on Mn removal efficiency in a calcite contactor with SFW containing a) 0.5 mg Mn L^{-1} (column A) and b) 5 mg Mn L^{-1} (column B)

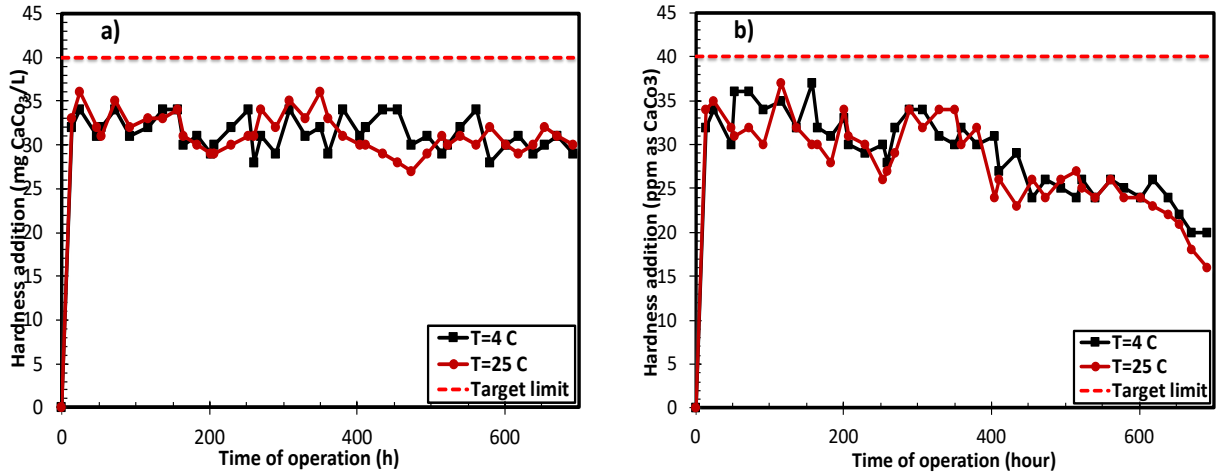

Figure 5-4: Temperature effect on efficiency of a calcite contactor in remineralization of soft SFW containing a) 0.5 mg Mn L^{-1} (column A) and b) 5 mg Mn L^{-1} (column B)

5.3 Impact of mixed beds (calcite/MgO) on Mn removal and hardness release

5.3.1 Identification of Calcite/ *Corosex*^{TM} ratio to maximise hardness release

Three different ratios of Calcite/*Corosex*^{TM} (90%:10%, 80%:20%, and 70%:30%) were tested in the first phase to find an optimum ratio regarding remineralization because the main objective of this section was to solve the problem of remineralization which was a limiting factor in the section 3.2.1.1 when only calcite was used. After having chosen the optimum ratio of 80/20 for Calcite/*Corosex*^{TM}, the same experiment as section 3.2.1.2 was undertaken to investigate the

efficiency of the contactor in remineralization of soft water with simultaneous Mn removal. Figure 5.5. demonstrates the results obtained from this experiment. Although the 70%:30% ratio releases slightly more hardness than 80%:20% ratio, the effluent pH in this case is too high for drinking water applications (pH=11.0). Health Canada suggest a maximum high pH value of 10.5 for drinking water consumption. As can be seen, 80%:20% ratio yielded better results in terms of the amount of hardness released to the water which is close to the predefined target limit and the effluent pH is still acceptable for drinking water purposes (pH=10); therefore, 80%:20% ratio was chosen for the next step.

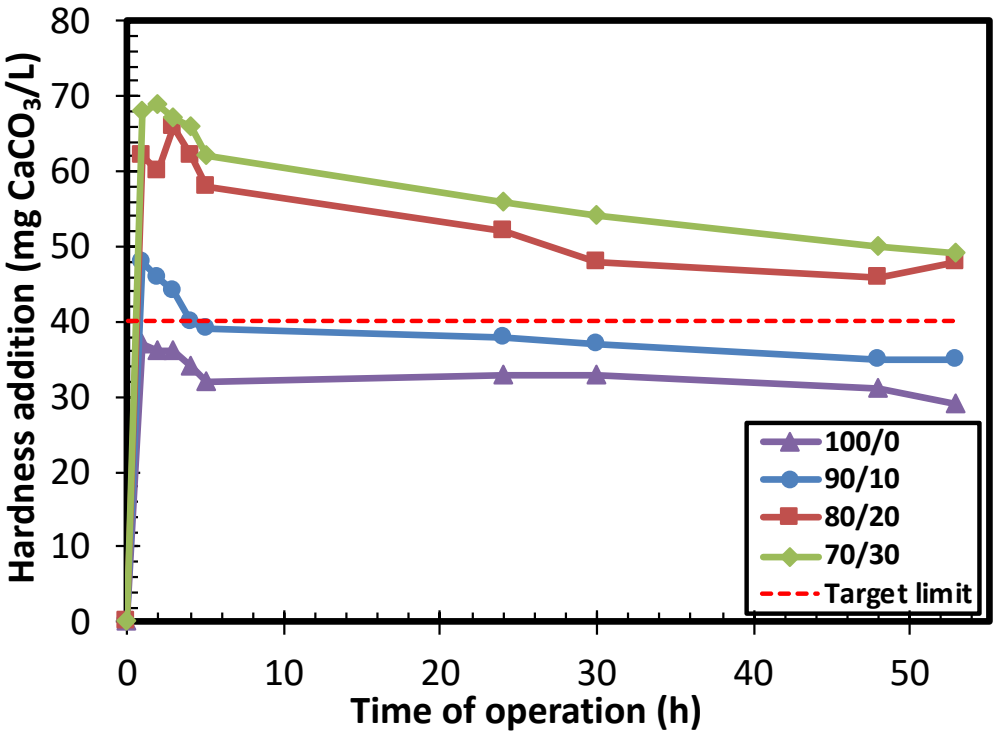

Figure 5-5: Hardness addition profile for four ratios of Calcite/ *Corosex*^{TM}, Feed had no Mn and no hardness, EBCT = 10 m, pH_{feed} = 6.0 and T = 23 °C

5.3.2 Sorption-dissolution experiments with a blend of calcite and *Corosex*^{TM}

Figure 5.6 presents the Mn^{2+} concentration profiles of the calcite contactor for SFW containing 5 mg Mn^{2+} L^{-1} in a long-term operation. The contactor was able to decrease the dissolved Mn from the SFW to below 20 µg Mn^{2+}/L. The stable condition was reached after 10 hours of operation which is much sooner than the case of using only calcite as the filter media (>200 h). The most crucial finding of this experiment was that both objectives (Mn removal and hardness increase) were met until approximately 600 hours of operation. However, clogging of the mixed media was noted because the pH was higher than in the case where only calcite was utilized (10.0-10.5). This

condition led to a faster Mn removal at the entry (i.e. bottom of the column) which led to the formation of a visible solid residue that overtime led to filter clogging (as shown in Fig. 5.7). It is of interest to point out that, with naked eye, a significant change of the color at the bottom of the bed treating SFW with 5 mg Mn^{2+} L^{-1} was observed (from milk-white towards black) as shown in Fig. 5.8. This change of color was more intense and more localized than when a pure bed of calcite was employed.

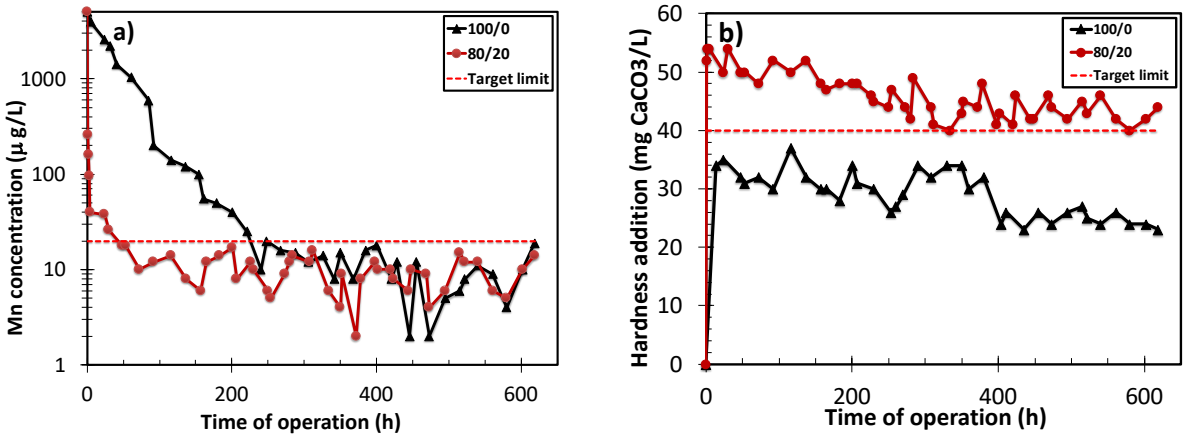

Figure 5-6: Performance figure of a calcite/ *Corosex*^{TM} contactor a) Mn^{2+} concentration profile, b) hardness addition profile

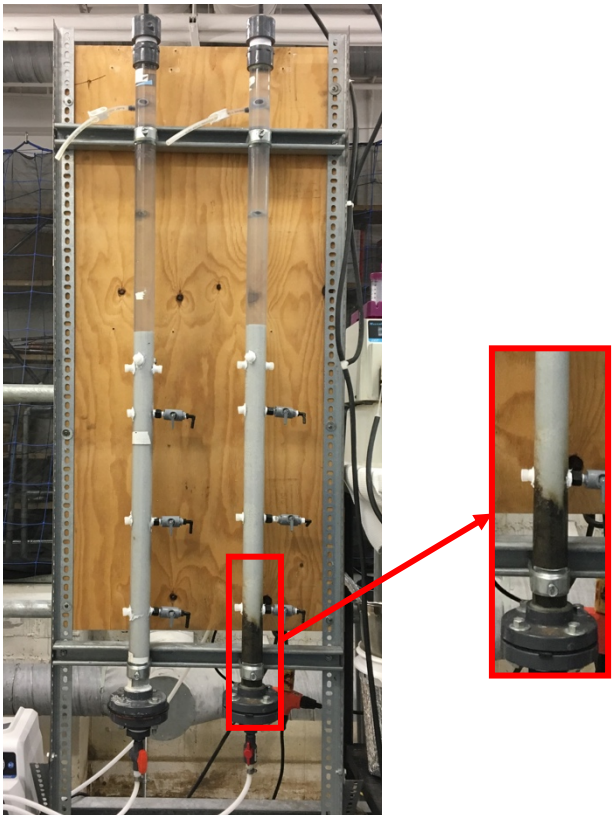

Figure 5-7: Experimental setup of calcite contactor (left column: control column running in parallel with the main column)

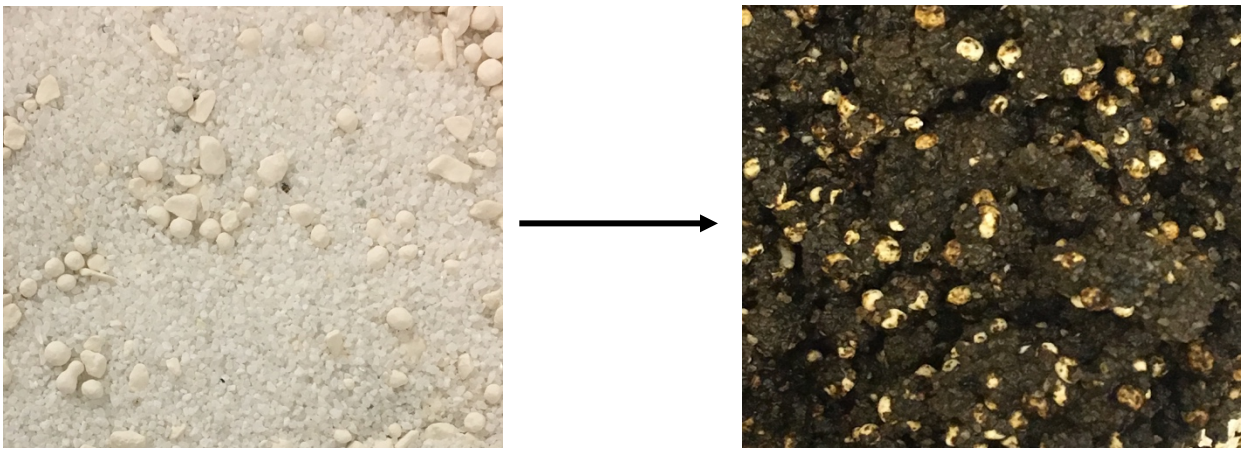

Figure 5-8: Comparison of a calcite/ *Corosex*^{TM} blend before and after a long-term operation of the contactor: left) virgin media, right) media after approximately 600 h of operation with Mn_i=5 mg/L

5.4 Conclusion

The main findings of the results of this chapter can be summarized as follow:

- An EBCT=10 minutes is sufficient for both Mn removal and remineralization.
- Temperature does not have a significant effect on Mn removal and calcite dissolution.
- 80% calcite:20% *Corosex*^{TM} ratio offered higher efficiency regarding the amount of hardness released to the water.
- When a blend of calcite and *Corosex*^{TM} was used, due to high pH condition (pH=10.0), a faster Mn removal was observed which suggests the precipitation of Mn as $Mn(OH)_2$.

Chapter 6 **GENERAL DISCUSSION**

This chapter highlights the main findings of this study. The main objective of this research effort was to develop a robust and compact process for simultaneous manganese removal and hardness adjustment of soft water for domestic applications, which can consistently guarantee the desired target limit in treated water (20 μg Mn^{2+}/L and 40 mg $CaCO_3$/L of hardness). To achieve this goal, we investigated: 1) the possibility of using calcite contactor for partial Mn removal and hardness level adjustment of treated water; 2) the coating effect of Mn on calcite dissolution rate; 3) modeling the long-term performance of a calcite contactor which is operated for the above-mentioned purposes; and 4) proposing a media blend (calcite and *Corosex*^{TM}) to achieve the target limit for remineralization. The main findings of each part are discussed in chapters 4 and 5.

6.1 Calcite contactor process for Mn removal and hardness adjustment

Short-term (4 hours) performance of calcite contactor for soft water remineralization with simultaneous Mn(II) removal was evaluated under different conditions (i.e., several iterations with varying initial Mn(II) concentration, Temperature, EBCT, etc.). As for manganese, the results demonstrated almost complete removal (below 20 μg Mn^{2+} L^{-1} in the effluent stream). Regarding remineralization, up to 40 mg $CaCO_3$/L of hardness addition was observed after an hour contact time. The Mn removal profiles were stable under low initial Mn concentrations (< 1.0 mg Mn^{2+}/L). However, under elevated Mn concentrations (>1.0 mg Mn^{2+}/L), an unstable Mn removal profile was observed especially for concentrations above 2.0 mg Mn^{2+} L^{-1}. Assays with varying EBCT and temperature were realized. For the tested conditions, an EBCT=10 min was selected as the optimum contact time required to have both remineralization and Mn removal to an acceptable extent (below 20 μg Mn^{2+} L^{-1} and over 40 mg $CaCO_3$/L of hardness addition to SFW) which is in good agreement with the findings of (Bang, 2012; Ghanbari, 2018; Nikolay, 2012). Short-term experiments were followed by long-term evaluation of the contactor to determine if the desired target limit in treated water can be consistently guaranteed. For this purpose, long-term (approximately 800 hours of operation) performance of the contactor was examined under different conditions. The Mn removal profile was stabilized after approximately 200 hours of operation and demonstrated high efficiency and consistency as short-term experiments but after 600 hours of operation under elevated Mn concentrations (5.0 mg Mn^{2+}/L), a decline in hardness addition was observed. It is worth mentioning that no significant change in the color of the bed treating SFW with 0.5 mg L^{-1} Mn^{2+} was observed visually. In contrary, feeding the filer with an SFW of 5 mg L^{-1} Mn^{2+} resulted in a significant change of the color of the bed (from milk-white towards black-brownish). These observations could be explained by the fact that at low Mn^{2+} concentrations at calcite surface, Mn incorporates mainly into the calcite matrix to form $MnCO_3$ and no discrete phase is formed at the surface, but at higher concentrations, $MnCO_3$ nucleation (slow growth phase of $MnCO_3$) (McBride, 1979) is followed by a slow recrystallization of $MnCO_3$ into MnO_2. In fact, at low aqueous concentrations, metals only incorporate into the calcite matrix by adsorption with no solid solution

formation (Comans & Middelburg, 1987; Franklin & Morse, 1983; McBride, 1979; Zachara et al., 1991) and this can explain the negligible color transformation throughout the bed for low concentration of Mn.

Of interest for the routine operation of the contactors, we investigated the Mn desorption rate by feeding, for 120 h with ultrapure water, the column with a high preloading of Mn. Effluent samples were collected frequently and analyzed for their Mn content. Results demonstrated no significant back dissolution of Mn to the aqueous phase; the Mn deposit formed appears very stable.

6.2 Mn Coating effect on calcite dissolution

Once the remineralization breakthrough was observed, filter media were collected for further investigation. After having transferred the contents of the highly loaded column (the column fed with SFW with 5 mg Mn^{2+} L^{-1}) to 4 smaller columns, the impact of Mn loading on calcite dissolution was investigated. It was observed that as the Mn loading increased from 1 to 15 mg Mn^{2+}/g calcite, the amount of hardness release gradually diminished. This phenomenon can be linked to the coating effect of Mn on calcite surface (Fig. 4.3), which inhibits the dissolution of calcite. According to the results of EDX analysis, from mini-columns 1 to 5, the Mn content on the calcite surface was gradually increased during long-term operation. Thereby, it can be assumed that an Mn layer is formed in the solid-liquid interface where the calcite dissolution reaction takes place and, accordingly, deteriorates the calcite dissolution. As mentioned earlier, the higher the Mn content in the calcite matrix, the lower the calcite dissolution is.

The literature review suggests the formation of $MnCO_3$ at calcite surface but one of the important differences of this research effort with previous works (McBride, 1979; Silva et al., 2012) is in the time of operation of the contactor. When the contactor operates for a long time (>600 hours), the effect of accumulated Mn on dissolution reaction is inevitable. A number of researchers reported the incorporation of Mn into calcite matrix and formation of $MnCO_3$ (Pingitore et al., 1988; Silva et al., 2012; Silva et al., 2010; Silva et al., 2012); however, based on the results of XPS analysis, the newly formed residue is not utterly $MnCO_3$ as the presence of Mn oxides and hydroxides were detected on the calcite surface. According to the fact that the analyzed depth in XPS is <10 nm (see appendix A), the observed Mn oxides and hydroxides are at the surface. These hypotheses were perfectly fitted into the proposed model with good reproduction of experimental data. The Mn sorption starts with an ion exchange reaction between soluble Mn^{2+} from the aqueous phase and Ca^{2+} from the $CaCO_3$ matrix which is followed by slow recrystallization of $MnCO_3$ into MnO_2.

As a concluding remark on this issue, it is important to point out that the coating effect was mostly discernable when the Mn concentration in the feed water was very high (5 mg Mn^{2+} L^{-1}). For the Mn concentrations expected in the permeate of the HFNF process (< 200 µg/L), it is anticipated that a 10 mg $CaCO_3$/L decline in hardness release would require at least 15,000 h of operation (1.7 years).

6.3 Modeling the long-term performance of a calcite contactor for Mn removal and remineralization via PHREEQC

A simple calcite dissolution rate based on calcite saturation index was defined which has been successfully used in previous modeling applications of phosphorus precipitation in packed bed contactors (Claveau-Mallet et al., 2017). As mentioned earlier, in low Mn concentration (i.e., 0.5 mg Mn^{2+}/L) in the feed, $MnCO_3$ formation by an ionic exchange between Ca^{2+} and Mn^{2+} takes place. In the elevated Mn concentration (i.e., 5 mg Mn^{2+}/L), Mn^{2+} is sorbed to the surface ($MnCO_3$ formation) then followed by slow recrystallization of $MnCO_3$ into MnO_2. The formation of MnO_2 was assumed according to mineralogical observations performed in this study (presented in the result section). The $MnCO_3$ precipitation rate was set as a first order reaction without $MnCO_3$ saturation assuming that autocatalytic sorption is taking place onto previously formed seeds. The $MnCO_3$ precipitation kinetic constant was slowly increasing to account for the increase of seeds. The simulated Mn molar repartition in the whole filter was 10% as MnO_2 and 90% as $MnCO_3$ in the $CaCO_3$ matrix. The calibration work resulted in a good reproduction of experimental data for both pH and manganese. The model captured the hardness decrease, though the simulated decrease slope was slightly smoother than the experimental one. Consequently, calcite dissolution was presumed to be progressively limited by the formation of a thin MnO_2 film over the surface of calcite grains. The diffusion of Ca^{2+} and CO_3^{2-} ions through the film was modeled based on Fick's law. At each iteration step, both dissolution and diffusion rates were calculated, and the smallest rate was applied only, which resulted in dissolution control at first and diffusion control afterward.

6.4 Blend of Calcite/ *Corosex™* media application

After long-term operation of the contactor in elevated Mn concentrations, the remineralization objective was not fully met when solely calcite was used. Hence, a possible solution was to use a blend of calcite and another media which contributes to the hardness adjustment objective and possibly does not interfere with the Mn removal objective. *Corosex™* (MgO) contributes to the water hardness adjustment by adding Mg ions to the water. For this purpose, three different ratios of Calcite/*Corosex™* were examined to find an optimum ratio and after having chosen the optimum ratio of 80% / 20% for Calcite/*Corosex™*, the column was operated under elevated Mn concentration (5 mg Mn^{2+} L^{-1}) to investigate the efficiency of the contactor in remineralization of soft water with simultaneous Mn removal. The column demonstrated high efficiency: the contactor was able to decrease the Mn concentration to below 20 µg Mn^{2+} L^{-1} and added above 40 mg/L as $CaCO_3$ hardness to the soft feed. The stable condition was reached much sooner than the previous experiment when only calcite was used (10 h of operation versus above 200 h of operation). The most crucial finding of this experiment was that the contactor perfectly added approximately 40 mg/L as $CaCO_3$ hardness to the SFW. Given that the pH was high (around 10), the introduced Mn was mostly captured at the very bottom of the bed. Accordingly, the filter bed started to be clogged after approximately 600 hours of operation mainly due to the impact of Mn precipitation resulting

from the high pH. Accumulation of newly formed Mn residue increased the head loss overtime and caused filter clogging. It is important to note that using a blend of calcite and *Corosex*^{TM} does not seem like a promising option for long-term operation if the Mn concentration in the feed is unrealistically high (i.e. 5 mg Mn^{2+} L^{-1}). However, for more realistic Mn concentrations (i.e. 0.2 mg Mn/L and less), adding a small portion of MgO to the filter would help improve the hardness addition. Given the high pH in the effluent, it might be enough to use 90% calcite: 10% *Corosex*^{TM}. In addition, epidemiological studies have documented the health benefits of Mg intake on cardiac health; Mg is a cofactor for several cellular enzymes, many of which are involved in the energy metabolism. Therefore, blending *Corosex*^{TM} (MgO) with calcite would also provide the added benefit of increasing the magnesium content of the finished water ((WHO), 2011; Health-Canada, 1979).

Chapter 7 CONCLUSIONS AND RECOMMENDATIONS

The primary purpose of this research project was to design a calcite contactor for simultaneous remineralization and manganese control for domestic applications. The following conclusions were derived from different parts of this research:

- **Long-term performance of a calcite contactor**

Calcite contactor fed with low Mn concentrations (< 0.5 mg Mn^{2+} L^{-1}) can operate for over 800 h while adding 30 mg $CaCO_3$/L of hardness and reducing the Mn below 20 µg/L in the treated water (i.e. the aesthetic objective). If the Mn concentration is increased to 5 mg Mn^{2+} L^{-1}, its removal will be unimpacted, even after 800 h of operation. However, after 600 h of operation (650 bed volumes), a decline in hardness release shall be expected due to the negative effect of Mn coating on the dissolution of calcite.

- **Potential release of Mn from Mn-loaded calcite media**

Mn desorption rate was investigated by feeding for 120 h with ultrapure water a calcite media preloaded with Mn at concentrations up to 15 mg Mn/g of media. Results demonstrated no significant back dissolution of Mn to the aqueous phase; thereby the formed Mn deposits are very stable.

- **Impact of Mn loading on calcite dissolution**

The higher the Mn content sorbed to the surface of calcite, the lower is the calcite dissolution and, subsequently, the lower is the hardness release. Fresh calcite (0 mg Mn/g calcite) exhibits higher hardness release than the Mn loaded calcite (1-15 mg Mn/g calcite). Sorption experiments, XPS and EDX analyses showed that hardness decline was most likely due to the MnOx present on the calcite surface. This phenomenon was linked to the coating effect of Mn on the calcite surface which inhibits the dissolution of calcite. We suggested that an Mn layer was formed in the solid-liquid interface where the dissolution reaction took place and, accordingly, deteriorated the calcite dissolution. With a low Mn concentration feed, Mn will only incorporate into the calcite matrix to form $MnCO_3$ and no significant discrete phase is formed at the surface. At higher Mn concentrations, $MnCO_3$ nucleation is followed by a slow recrystallization of $MnCO_3$ into MnO_2. The conclusion can explain the negligible color transformation throughout the bed for low concentration of Mn as opposed to the development of a black-brownish color in the column fed with 5 mg Mn/L.

- **Simulation of long-term operation of calcite contactors**

The implemented modelling strategy consisted of two steps: (i) fast Mn removal by sorption and (ii) slow crystallization of $MnCO_3$ as MnO_2. Including this last step was essential to properly model the observed pH behaviour of the effluent because the pH at the effluent was predicted to be highly influenced by the recrystallization rate. The fastest recrystallization rates resulted in an

unrealistically low pH (<6.5 at 5000 µg Mn^{2+} L^{-1}). Indeed, the simulated MnO_2 proportion in Mn precipitate for the column fed with 5 mg Mn L^{-1} was over 10%, which was sufficient to be detected by XPS analysis.

- **Long-term performance of a calcite/*Corosex™* column**

Since a decline in hardness release was observed after 600 h of operation in the first phase, a solution was tested to resolve this issue. The addition of MgO to the calcite media contributes to the water hardness adjustment by adding Mg ions to the water and also contributes to Mn removal by raising the pH around 10 where the rate of manganese precipitation is increased. It is shown that the optimum ratio is 80% clacite/20% *Corosex™*. The column exhibited high efficiency: the contactor was able to reduce the Mn concentration to below 20 µg Mn^{2+}/L in the effluent and added above 40 mg $CaCO_3$/L of hardness to the soft feed. Given that the pH was high (around 10), the introduced Mn was mostly captured at the very bottom of the bed. For realistic feed Mn concentrations (i.e. 0.2 mg/L and less), this option could also be appealing because of the documented health benefits of Mg intake on cardiac health. However, it does not seem to be a promising option for long-term operation if the Mn concentration in the feed is unrealistically high (i.e. 5 mg L^{-1} Mn^{2+}) due to the excessive precipitation of $Mn(OH)_2$ expected at the bottom of the columen.

This work inspired the following ideas for future studies. It would be interesting to:

- Evaluate the contactor performance for removal of other heavy metals that are frequently present in groundwater such as iron which naturally co-exists with manganese in high concentrations.
- Develop a model for calcite/*Corosex™* column to predict the long-term behavior of the contactor.
- Evaluate the long-term performance of the HFNF-calcite contactor in a pilot-scale study using natural groundwater.

BIBLIOGRAPHY

(WHO), W. H. O. (2011). *Hardness in Drinking-water: WHO Guidelines for Drinking-water Quality*. World Health Organization, Geneva, Switzerland:

Arvidson, R. S., Collier, M., Davis, K. J., Vinson, M. D., Amonette, J. E., & Luttge, A. (2006). Magnesium inhibition of calcite dissolution kinetics. *Geochimica et Cosmochimica Acta, 70*(3), 583-594. doi:https://doi.org/10.1016/j.gca.2005.10.005

Aziz, H. A., & Smith, P. G. (1992). The influence of pH and coarse media on manganese precipitation from water. *Water Research, 26*(6), 853-855. doi:https://doi.org/10.1016/0043-1354(92)90017-X

Aziz, H. A., & Smith, P. G. (1996). Removal of manganese from water using crushed dolomite filtration technique. *Water Research, 30*(2), 489-492. doi:https://doi.org/10.1016/0043-1354(95)00178-6

Baer, D. R., Blanchard, D. L., Engelhard, M. H., & Zachara, J. M. (1991). The interaction of water and Mn with surfaces of CaCO3: An XPS study. *Surface and Interface Analysis, 17*(1), 25-30. doi:doi:10.1002/sia.740170108

Bang, D. P. (2012). *Upflow limestone contactor for soft and desalinated water.* (Delft University of Technology, Delft, Netherland).

Barbeau, B., Carrière, A., & Bouchard, M. F. (2011). Spatial and temporal variations of manganese concentrations in drinking water. *Journal of Environmental Science and Health, Part A, 46*(6), 608-616. doi:10.1080/10934529.2011.562854

Benefield, L. D., Judkins, J. F., & Weand, B. L. (1982). *Process Chemistry for Water and Wastewater Treatment*. Englewood Cliffs: Prentice-Hall.

Bouchard, M. F., Sauvé, S., Barbeau, B., Legrand, M., Brodeur, M.-È., Bouffard, T., . . . Mergler, D. (2011). Intellectual impairment in school-age children exposed to manganese from drinking water. *Environmental health perspectives, 119*(1), 138.

Carrière, A., Brouillon, M., Sauvé, S., Bouchard, M. F., & Barbeau, B. (2011). Performance of point-of-use devices to remove manganese from drinking water. *Journal of Environmental Science and Health, Part A, 46*(6), 601-607. doi:10.1080/10934529.2011.562852

Charlton, S. R., & Parkhurst, D. L. (2011). Modules based on the geochemical model PHREEQC for use in scripting and programming languages. *Computers & Geosciences, 37*(10), 1653-1663.

Civardi, J., & Tompeck, M. (2015). *Iron and Manganese Removal Handbook*: American Water Works Association.

Claveau-Mallet, D., Courcelles, B., Pasquier, P., & Comeau, Y. (2017). Numerical Simulations with the P-Hydroslag Model for Prediction of Phosphorus Removal by Steel Slag Filters. *Water Research, 126* 421-432.

Comans, R. N. J., & Middelburg, J. J. (1987). Sorption of trace metals on calcite: Applicability of the surface precipitation model. *Geochimica et Cosmochimica Acta, 51*(9), 2587-2591. doi:https://doi.org/10.1016/0016-7037(87)90309-7

Dion, L.-A., Saint-Amour, D., Sauvé, S., Barbeau, B., Mergler, D., & Bouchard, M. F. (2018). Changes in water manganese levels and longitudinal assessment of intellectual function in children exposed through drinking water. *NeuroToxicology, 64* 118-125. doi:https://doi.org/10.1016/j.neuro.2017.08.015

Domenico, P. A., & Schwartz, F. W. (1998). *Physical and Chemical Hydrogeology* (2 ed.). New York: John Wiley & sons.

Erga, O. T., S. G. (1956). Kinetics of the Heterogeneous Reaction of Calcium Bicarbonate Formation, with Special Reference to Copper Ion Inhibition. *Acta Chemica Scandinavica 1947 - 1999* 872-874. doi:10.3891/acta.chem.scand.10-0872

Farley, K. J., Dzombak, D. A., & Morel, F. M. M. (1985). A surface precipitation model for the sorption of cations on metal oxides. *Journal of Colloid and Interface Science, 106*(1), 226-242. doi:https://doi.org/10.1016/0021-9797(85)90400-X

Fogler, H. S. (1999). *Elements of chemical reaction engineering*: Third edition. Upper Saddle River, N.J. : Prentice Hall PTR, [1999] ©1999.

Franklin, M. L., & Morse, J. W. (1983). The interaction of manganese(II) with the surface of calcite in dilute solutions and seawater. *Marine Chemistry, 12*(4), 241-254. doi:https://doi.org/10.1016/0304-4203(83)90055-5

Gambou-Bosca, A., & Bélanger, D. (2016). Electrochemical accessibility of porous submicron MnO2 spheres as active electrode materials for electrochemical capacitors. *Electrochimica Acta, 201* 20-29. doi:https://doi.org/10.1016/j.electacta.2016.03.108

Ghanbari, S. (2018). *Pilot study and modeling of remineralization of low-temperature desalinated water by calcite filtration.* (Delft University of Technology, Delft, Delft).

Haddad, M., Ohkame, T., Bérubé, P. R., & Barbeau, B. (2018). Performance of thin-film composite hollow fiber nanofiltration for the removal of dissolved Mn, Fe and NOM from domestic groundwater supplies. *Water Research, 145* 408-417. doi:https://doi.org/10.1016/j.watres.2018.08.032

Health-Canada. (1979). *Guidelines for Canadian Drinking Water Quality: Guideline Technical Document – Manganese*.

Health-Canada. (2016). *Manganese in drinking water. Federal-Provincial-Territorial Committee on Drinking Water*.

Hernández-Suárez, M. (2005). *Short Guideline For Limestone Contactor Design For Large Desalination Plants*. Canary Islands Water Center:

Kenari, S. L. D. (2017). *Integrated Fluidized Bed-Membrane Process for Advanced Iron and Manganese Control in Drinking Water.* (École Polytechnique de Montréal).

Kothari, N. (1988). Groundwater, iron and manganese an unwelcome trio. *Water Engineering and Management; (USA)* Medium: X; Size: Pages: 25-26.

Kozisek, F. (2004). *Health risks from drinking demineralised water*. National Institute of Public Health Czech Republic: World Health Organisation (WHO)

Lehmann, O., Birnhack, L., & Lahav, O. (2013). Design aspects of calcite-dissolution reactors applied for post treatment of desalinated water. *Desalination, 314* 1-9. doi:https://doi.org/10.1016/j.desal.2012.12.017

Letterman, R. D., Driscoll, C. T., Haddad, M., & Hsu, H. A. (1987). Limestone bed contactors for control of corrosion at small water utilities. In *Limestone bed contactors for control of corrosion at small water utilities*: US EPA. Water Engineering Research Laboratory.

Letterman, R. D., Hadad, M., & Driscoll, C. T. (1991). Limestone Contactors: Steady State Design Relationships. *Journal of Environmental Engineering, 117*(3), 339-358. doi:doi:10.1061/(ASCE)0733-9372(1991)117:3(339)

McBride, M. B. (1979). Chemisorption and Precipitation of Mn2+ at CaCO3 Surfaces1. *Soil Science Society of America Journal, 43*(4), 693-698. doi:10.2136/sssaj1979.03615995004300040013x

Mettler, S., Wolthers, M., Charlet, L., & Gunten, U. v. (2009). Sorption and catalytic oxidation of Fe(II) at the surface of calcite. *Geochimica et Cosmochimica Acta, 73*(7), 1826-1840. doi:https://doi.org/10.1016/j.gca.2009.01.003

Morse, J. W., Arvidson, R. S., & Lüttge, A. (2007). Calcium Carbonate Formation and Dissolution. *Chemical Reviews, 107*(2), 342-381. doi:10.1021/cr050358j

Nikolay, V. (2012). *Desalination Engineering: Planning and Design*: McGraw-Hill Professional.

Omri, A., & Benzina, M. (2012). Removal of manganese(II) ions from aqueous solutions by adsorption on activated carbon derived a new precursor: Ziziphus spina-christi seeds. *Alexandria Engineering Journal, 51*(4), 343-350. doi:https://doi.org/10.1016/j.aej.2012.06.003

Parkhurst, D. L., & Appelo, C. A. J. (1999). *User's guide to PHREEQC (Version 2) - A computer program for speciation, batch-reaction, one-dimensional transport, and inverse geochemical calculations* (Publication No. Water-Resources Investigations Report 99-4259). Denver:

Pingitore, N. E., Eastman, M. P., Sandidge, M., Oden, K., & Freiha, B. (1988). The coprecipitation of manganese(II) with calcite: an experimental study. *Marine Chemistry, 25*(2), 107-120. doi:https://doi.org/10.1016/0304-4203(88)90059-X

Plummer, L., Parkhurst, D., & Wigley, T. (1979). Critical review of the kinetics of calcite dissolution and precipitation. In: ACS Publications.

Plummer, L., Wigley, T., & Parkhurst, D. (1978). The kinetics of calcite dissolution in CO 2-water systems at 5 degrees to 60 degrees C and 0.0 to 1.0 atm CO 2. *American journal of science, 278*(2), 179-216.

Ruggieri, F., Fernandez-Turiel, J. L., Gimeno, D., Valero, F., García, J. C., & Medina, M. E. (2008). Limestone selection criteria for EDR water remineralization. *Desalination, 227*(1), 314-326. doi:https://doi.org/10.1016/j.desal.2007.07.020

Shemer, H., Hasson, D., & Semiat, R. (2013). Design Considerations of a Packed Calcite Bed for Hardening Desalinated Water. *Industrial & Engineering Chemistry Research, 52*(31), 10549-10553. doi:10.1021/ie302975b

Shemer, H., Hasson, D., Semiat, R., Priel, M., Nadav, N., Shulman, A., & Gelman, E. (2012). *Remineralization of desalinated water by limestone dissolution with carbon dioxide* (Vol. 51).

Silva, A. M., Cordeiro, F. C. M., Cunha, E. C., & Leão, V. A. (2012). Fixed-Bed and Stirred-Tank Studies of Manganese Sorption by Calcite Limestone. *Industrial & Engineering Chemistry Research, 51*(38), 12421-12429. doi:10.1021/ie301752q

Silva, A. M., Cruz, F. L. S., Lima, R. M. F., Teixeira, M. C., & Leão, V. A. (2010). Manganese and limestone interactions during mine water treatment. *Journal of Hazardous Materials, 181*(1), 514-520. doi:https://doi.org/10.1016/j.jhazmat.2010.05.044

Silva, A. M., Cunha, E. C., Silva, F. D. R., & Leão, V. A. (2012). Treatment of high-manganese mine water with limestone and sodium carbonate. *Journal of Cleaner Production, 29-30* 11-19. doi:https://doi.org/10.1016/j.jclepro.2012.01.032

Sly, L. I., Hodgkinson, M. C., & Arunpairojana, V. (1990). Deposition of manganese in a drinking water distribution system. *Applied and Environmental Microbiology, 56*(3), 628-639. Retrieved from https://aem.asm.org/content/aem/56/3/628.full.pdf

Thornton, F. C. (1995). Manganese removal from water using limestone-filled tanks. *Ecological Engineering, 4*(1), 11-18. doi:https://doi.org/10.1016/0925-8574(94)00003-N

Tobiason, J. E., Bazilio, A., Goodwill, J., Mai, X., & Nguyen, C. (2016). Manganese Removal from Drinking Water Sources. *Current Pollution Reports, 2*(3), 168-177. doi:10.1007/s40726-016-0036-2

USEPA. (2004). *United States Environmental Protection Agency (USEPA). Drinking water health advisory for manganese.* Health and Ecological Criteria Division, Washington, DC, USA (pp. 55):

Van Der Laan. H., V. O. J., Van Houwelingen. G., Sousi. M., Zijp. M., Kok. L., Schoonderwoerd. V. (2016). *Search for the optimal remineralization technology.* South Holland: Delft University of Technology.

W. Walker, W. Y. S., Justin Sutherland, Bradley Sessions, Erin Mackey,. (2012). *Upflow Calcite Contactor Study*. Texas Water Development Board:

Walker, W. S. (2012). *Upflow Calcite Contactor Study*. University of Texas at El Paso: Texas Water Development Board Contract #1004831105

Wen, X., Du, Q., & Tang, H. (1998). Surface Complexation Model for the Heavy Metal Adsorption on Natural Sediment. *Environmental Science & Technology, 32*(7), 870-875. doi:10.1021/es970098q

Wersin, P., Charlet, L., Karthein, R., & Stumm, W. (1989). From adsorption to precipitation: Sorption of Mn2+ on FeCO3(s). *Geochimica et Cosmochimica Acta, 53*(11), 2787-2796. doi:https://doi.org/10.1016/0016-7037(89)90156-7

Withers, A. (2005). Options for recarbonation, remineralisation and disinfection for desalination plants. *Desalination, 179*(1), 11-24. doi:https://doi.org/10.1016/j.desal.2004.11.051

Yamauchi, V., Tanaka, K., Hattori, K., Kondo, M., & Ukawa, N. (1987). Remineralization of desalinated water by limestone dissolution filter. *Desalination, 66* 365-383.

Zachara, J. M., Cowan, C. E., & Resch, C. T. (1991). Sorption of divalent metals on calcite. *Geochimica et Cosmochimica Acta, 55*(6), 1549-1562. doi:https://doi.org/10.1016/0016-7037(91)90127-Q

APPENDIX A – MEDIA CHARACTERIZATION ANALYSES

1. Electron microscopy and elemental analysis

Scanning electron microscopy (SEM) images were taken at 250X magnification using a field emission gun electron microscope (model: JMS-7600 FEG-SEM, Jelo, USA). An energy dispersive spectrometer (model: Oxford X-Max silicon drift detector, Oxford Instrument, UK) was connected to the microscope to perform the elemental analysis of the surface of calcite media (EDX). The EDX analysis was carried out at the same magnification as the SEM analysis (250X), using a 15 kV accelerating voltage and a 20 mm working distance.

2. X-ray Photoelectron Spectrometry (XPS) analysis

X-ray Photoelectron Spectrometry (XPS) analysis was done on the surface of the fresh and Mn loaded calcite media. The experimental conditions of the XPS analysis are given in the following table.

Table A-1: Experimental conditions of XPS analysis

Operational conditions	**Data**
Apparatus	VG ESCALAB 3 MKII
Source	Al Kα
Power	300 W (15 kV, 20 mA)
Pressure in analysis chamber	3.0 x 10-9 Torr
Analysed surface	2 mm x 3 mm
Electron takeoff angle	0 degrees
Analysed depth	< 10 nm
Detection limit	~ 0.1 % atomic
Survey scans energy: step size	1.0 eV
Survey scans energy: pass energy	100 eV
High resolution scans: energy step size	0.05 eV

High resolution scans: pass energy	20 eV
Background subtraction	Shirley method
Sensitivity factor table	Wagner
Charge correction with respect to C1s at	285.0 eV